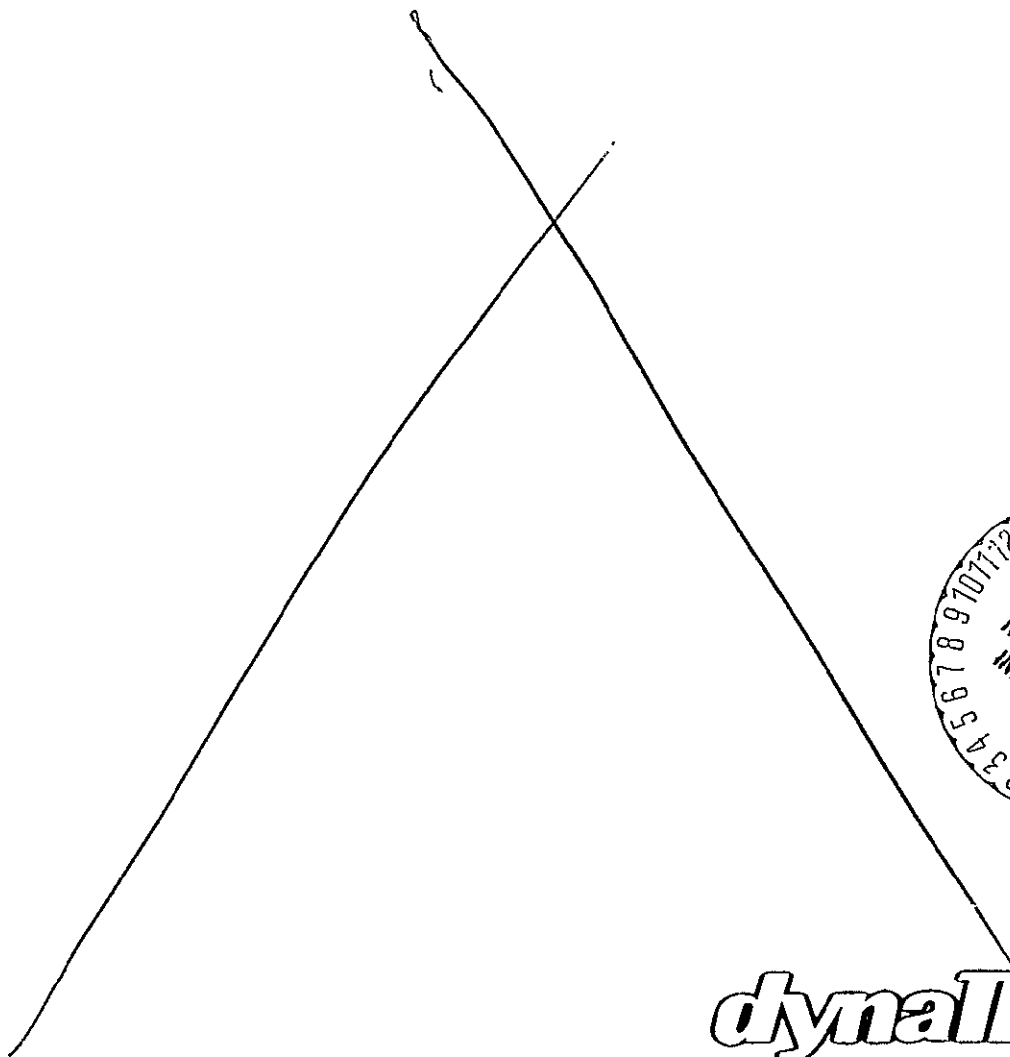


CR-152015

(NASA-CR-152015) DEVELOPMENT OF A JET PUMP-ASSISTED ARTERIAL HEAT PIPE Final Report (Dynatherm Corp., Cockeysville, Md.) 55 p HC A04/MF A01	N77-30415 CSCI 20D G3/34	Unclas 46207
--	------------------------------------	-----------------



dynaTherm
CORPORATION

N77-30415

DTM-77-2

FINAL REPORT

for

DEVELOPMENT OF A JET PUMP-ASSISTED
ARTERIAL HEAT PIPE

Walter B. Bienert
Amon S. Ducao
Donald S. Trimmer

May 6, 1977

Prepared Under Contract NAS2-9233

for

National Aeronautics and Space Administration
Ames Research Center
Moffett Field, California

REPRODUCED BY
NATIONAL TECHNICAL
INFORMATION SERVICE
U. S. DEPARTMENT OF COMMERCE
SPRINGFIELD, VA. 22161

by

Dynatherm Corporation
One Industry Lane
Cockeysville, Maryland

ABSTRACT

This report describes the development of a jet pump assisted arterial heat pipe. This new concept promises a solution to the problem of starting arterial heat pipes, in particular those using high pressure working fluids such as ammonia. The concept utilizes a built-in capillary driven jet pump to remove vapor and gas from the artery and to prime it. The continuous pumping action also prevents depriming during operation of the heat pipe. The concept is applicable to fixed conductance and gas loaded variable conductance heat pipes.

The report presents a theoretical model for the jet pump assisted arterial heat pipe. The model was used to design a prototype for laboratory demonstration. The 1.2 m long heat pipe was designed to transport 500 watts and to prime at an adverse elevation of up to 1.3 cm. The test results were in good agreement with the theoretical predictions. The heat pipe carried as much as 540 watts and was able to prime up to 1.9 cm. Introduction of a considerable amount of non-condensable gas had no adverse affect on the priming capability.

FOREWORD

This report presents the summary of the "Development of a Jet Pump Assisted Arterial Heat Pipe." The concept originated at Dynatherm and the development was funded by NASA-Ames Research Center under Contract NAS2-9233. NASA's Technical Monitor was Dr. Craig McCreight, whose continuing interest in this work is greatly appreciated.

TABLE OF CONTENTS

	<u>Page</u>
1. INTRODUCTION AND SUMMARY	1
2. PRINCIPLE AND THEORY OF JET PUMP ASSISTED PRIMING	2
2.1 Qualitative Description	2
2.2 Theory of Capillary Jet Pump	4
2.3 Interpretation of Performance Equations	10
2.4 Application of Analytical Model to Design of Heat Pipe	15
3. BENCH TESTS	19
3.1 Effects of Mass Injection on Jet Pump Performance	19
3.2 Required Rate of Mass Injection for Artery Priming	21
3.3 Pressure Losses Between Artery and Injection Port	24
3.4 Bench Test of Prototype Jet Pump	24
4. DESIGN OF JET PUMP ASSISTED ARTERIAL HEAT PIPE	28
4.1 Thermal Design	28
4.2 Mechanical Design	29
4.3 Test Setup	33
5. TEST RESULTS WITH JET PUMP ASSISTED HEAT PIPE	36
5.1 Deactivated Jet Pump	36
5.2 Jet Pump Assisted Artery	36
5.3 Jet Pump Assisted Artery with Noncondensable Gas	42
6. CONCLUSIONS AND RECOMMENDATIONS	46
7. REFERENCES	47

NOMENCLATURE

<u>Symbol</u>		<u>Unit</u>
A	Area	m^2
C	Conductance	m^4/sec
C_v	Inverse of lumped vapor resistance	m^4/sec
D	Diameter	m
K	Permeability	m^2
L	Effective length	m
N_l	Liquid transport factor of the working fluid	W/m^2
ΔP_{cap}	Capillary pumping pressure difference between liquid and vapor	N/m^2
ΔP_d	Vapor pressure loss across venturi	N/m^2
ΔP_{grav}	Gravity term	N/m^2
ΔP_l	Viscous pressure loss in the liquid	N/m^2
ΔP_n	Useful suction pressure of the venturi	N/m^2
ΔP_v	Vapor pressure loss across lumped vapor resistance	N/m^2
Q	Axial heat flow rate	W
g	Acceleration	m/sec^2
l	Length of primed portion of the artery	m
r_p	Effective pore radius of the wick	m
\dot{V}	Volumetric flow rate	Liter/min
α	Heat pipe orientation with respect to gravity	deg
η	Venturi efficiency	%
η_d	Diffuser efficiency	%

NOMENCLATURE (Cont'd)

<u>Symbol</u>		<u>Unit</u>
η_n	Nozzle efficiency	%
λ	Latent heat of evaporation	J/Kg
ρ	Density	Kg/m ³
σ	Surface tension	N/m
F	Proportionality constant defined by the ratio: $\frac{1}{2 \rho_v \lambda^2 A_t^2 \eta_n}$	
f	Normalized parameter defined by the ratio: $\frac{\Delta P_{cap}^-}{\Delta P_{cap, o}}$	
δ	Normalized parameter defined by the ratio: $\frac{\rho_l g L \sin \alpha}{\Delta P_{cap, o}}$	
γ	Normalized parameter defined by the ratio: $\frac{C_a + C_w}{C_w}$	
ϵ	Normalized parameter defined by the ratio: $\frac{\Delta P_{cap, a}}{\Delta P_{cap, o}}$	

NOMENCLATURE (Cont'd)

Subscripts

a	Artery
abs	Absolute
c	Condenser
d	Diffuser
e	Evaporator
l	Liquid
n	Nozzle
o	Denotes values at "0" g environment
t	Venturi throat
v	Vapor
w	Priming wick or wick
x	Axial coordinate

1. INTRODUCTION AND SUMMARY

This report describes the work performed by Dynatherm Corporation under Contract NAS2-9233. The program was initiated on June 3, 1976 and completed on May 2, 1977.

The present contract is a continuation of development initiated on Purchase Order Number A12056(MW). The goal of the previous program was to investigate a new concept for priming an artery in a heat pipe. This concept utilizes a capillary driven jet pump to create the necessary suction to fill the artery. A proof-of-principle experiment was performed which demonstrated that the jet pump had the ability to maintain a primed artery even against a substantial adverse gravity gradient.

Under the present contract, the concept was applied to a working model of an ammonia heat pipe. It was designed to transport 500 watts and to prime at adverse elevation up to 1.3 cm. Experiments with the heat pipe demonstrated operation in good agreement with predictions. The artery was able to prime reliably even after introducing a considerable amount of noncondensable gas into the heat pipe. The program has demonstrated that a jet-assisted arterial heat pipe can be designed to meet specific requirements and will function reliably. Using this concept, high axial transport can be achieved with an arterial variable conductance gas-controlled heat pipe. In the past, it was generally accepted (Ref. 1) that arteries are very difficult to prime or will not function at all in ammonia VCHP's.

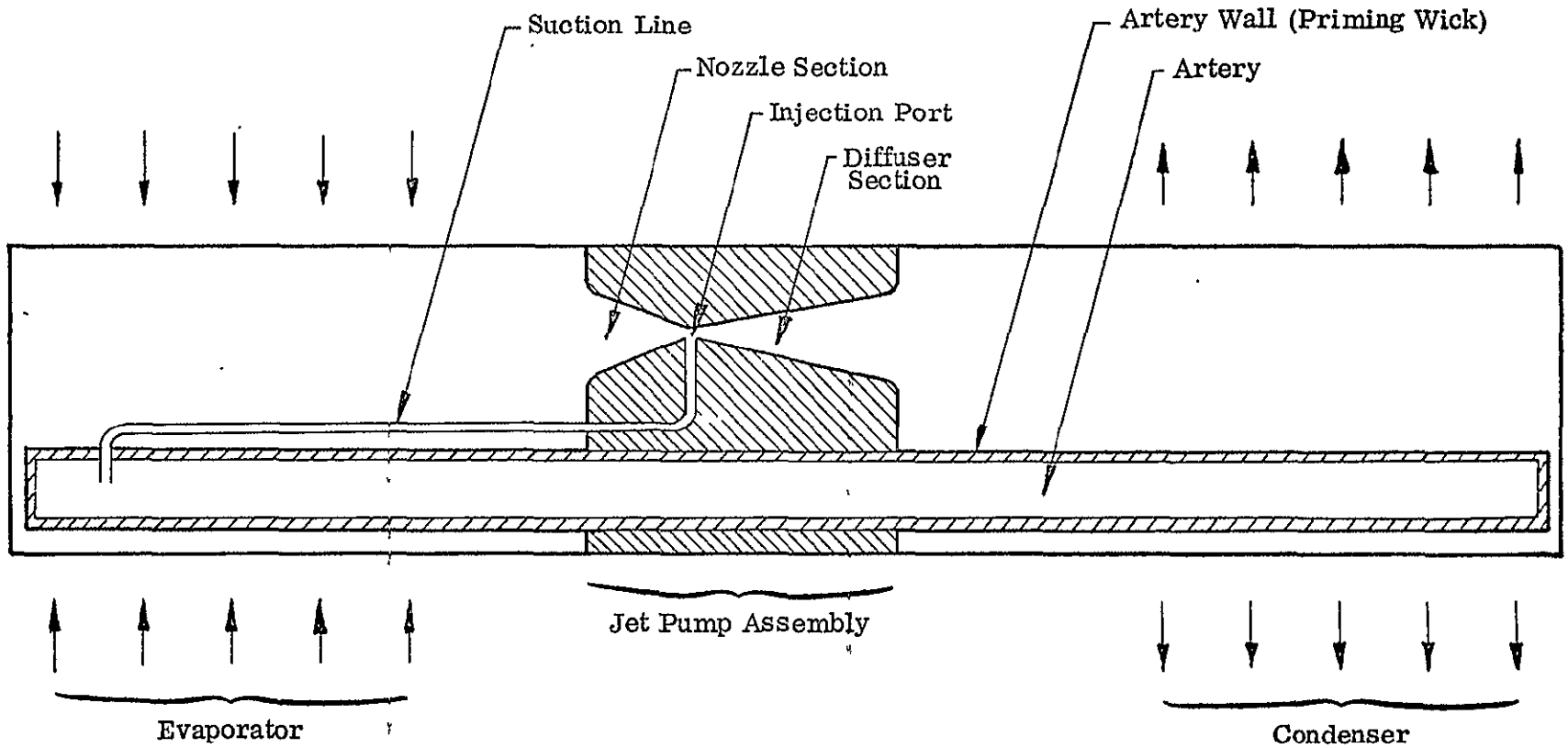
2. PRINCIPLE AND THEORY OF JET PUMP ASSISTED PRIMING

2.1 Qualitative Description

A schematic of a jet pump assisted arterial heat pipe is shown in Figure 2.1. The jet pump assembly consists of a venturi which separates the vapor in the evaporator from the vapor in the condenser. A suction line connects the end of the artery to an injection port at the throat of the venturi. In a conventional arterial heat pipe, the artery is designed to prime through capillary action alone. This requires that the artery has a small diameter (typically 3 mm for an NH_3 heat pipe), that no noncondensable gas is present, and that priming occurs before the full load is applied (the load could be either thermal or gravitational).

The capillary driven jet pump provides a more powerful priming mechanism. When a thermal load is applied to the heat pipe, the vapor flowing toward the condenser has to pass through the converging-diverging venturi. Acceleration of the vapor in the nozzle section causes its pressure to drop below the saturation pressure in the evaporator. The lowest pressure occurs at the throat; most of the pressure drop is recovered in the diffuser. Since the artery is connected to the throat, it "sees" the same reduced pressure which causes it to prime. The achievable suction pressure is a function of the throat area and the vapor flow rate. Unlike the conventional arterial heat pipe, the priming capability of the jet pump assisted artery increases with higher heat loads. The suction pressure also increases as the throat of the venturi becomes smaller. However, the pressure loss across the venturi, which must be overcome by the capillary pumping of the wick, sets a practical lower limit for the throat area. In addition to being able to prime under load, the jet pump is also unaffected by noncondensable gas. Finally, the suction pressures are sufficiently large to prime large diameter arteries which could not otherwise be primed in a one-g environment.

The following paragraphs give a more detailed but still qualitative description of the priming mechanism. The analytical model is presented in the next section. Since the jet pump needs a finite vapor flow to create a suction pressure, the artery must be paralleled by a "priming wick". Sometimes the permeability of the screen forming the artery suffices for this purpose. Suppose the artery is initially empty but the priming



131

FIGURE 2.1
SCHEMATIC OF JET PUMP ASSISTED ARTERIAL HEAT PIPE

wick is saturated. When heat is first applied, vapor begins to flow, but the viscous losses in the priming wick quickly reach the capillary limit. But even a small vapor flow creates a finite suction pressure to cause partial artery priming. The primed section of the artery "shorts" the priming wick and increases its effective permeability. This permits a further increase in power. If the design has been properly chosen, the power can be gradually increased until the entire artery is filled without ever exceeding the capillary limit. Beyond that point, the effective permeability of the artery-priming wick combination remains constant. But the heat load can still be increased until the capillary limit of the fully primed artery is reached. It is important to note that the jet pump assisted arterial heat pipe can operate in a stable manner with a partially primed artery. By contrast, a conventional arterial pipe has two stable modes of operation. When the artery is fully primed, the available capillary pumping is that of the closed artery. When the artery is deprimed (even by a small amount), its pumping capability is reduced to that of a capillary equal to the artery diameter.

2.2 Theory of Capillary Jet Pump

A mathematical model has been developed which describes the hydrodynamics of a jet pump assisted arterial heat pipe. The model uses the following simplifying assumptions:

- (1) The vapor flow is laminar, isothermal, and incompressible.
- (2) The viscous pressure drop in the vapor (except for the venturi) can be lumped into a single resistance.
- (3) The vapor follows the ideal gas law.
- (4) The performance of the jet pump is not affected by vapor, gas, or liquid pumped from the artery. (This assumption will be later justified through test results.)
- (5) Pressure losses in the suction tube are negligible.
- (6) The capillary stress in the condenser is zero (equal liquid and vapor pressure).
- (7) All heat inputs and outputs occur at the extreme ends of the heat pipe.

The usual pressure balance for the heat pipe is:

$$\Delta P_{\text{cap}} = \Delta P_1 + \Delta P_d + \Delta P_v + \Delta P_{\text{grav}} \quad (1)$$

where

ΔP_{cap} = capillary pumping pressure difference between liquid and vapor at the evaporator

ΔP_1 = viscous pressure loss in the liquid

ΔP_d = vapor pressure loss across venturi

ΔP_v = vapor pressure loss across lumped vapor resistance

ΔP_{grav} = gravity term

Figure 2.2 shows a schematic of the heat pipe with the artery partially primed. At any axial location, the liquid pressure in artery and priming wick must be identical:

$$P_{l,a}(x) = P_{l,w}(x) \quad (2)$$

In laminar flow, the viscous pressure gradients are related to the heat flow rate through an equivalent wick conductance C:

$$\frac{dp}{dx} = \frac{1}{C} Q \quad (3)$$

Thus, the pressure loss in the liquid becomes:

$$\Delta P_1 = \frac{1}{C_a + C_w} l Q + \frac{1}{C_w} (L - l) Q \quad (4)$$

In the last equation, C_a and C_w are the conductances of artery and wick, respectively. The first term on the right side of (4) represents the pressure drop in the primed section of the artery and the second term in the unprimed section.

The pressure drop of the vapor across the venturi can be expressed as follows (Ref. 2):

$$\Delta P_d = (1 - \eta) F Q^2 \quad (5)$$

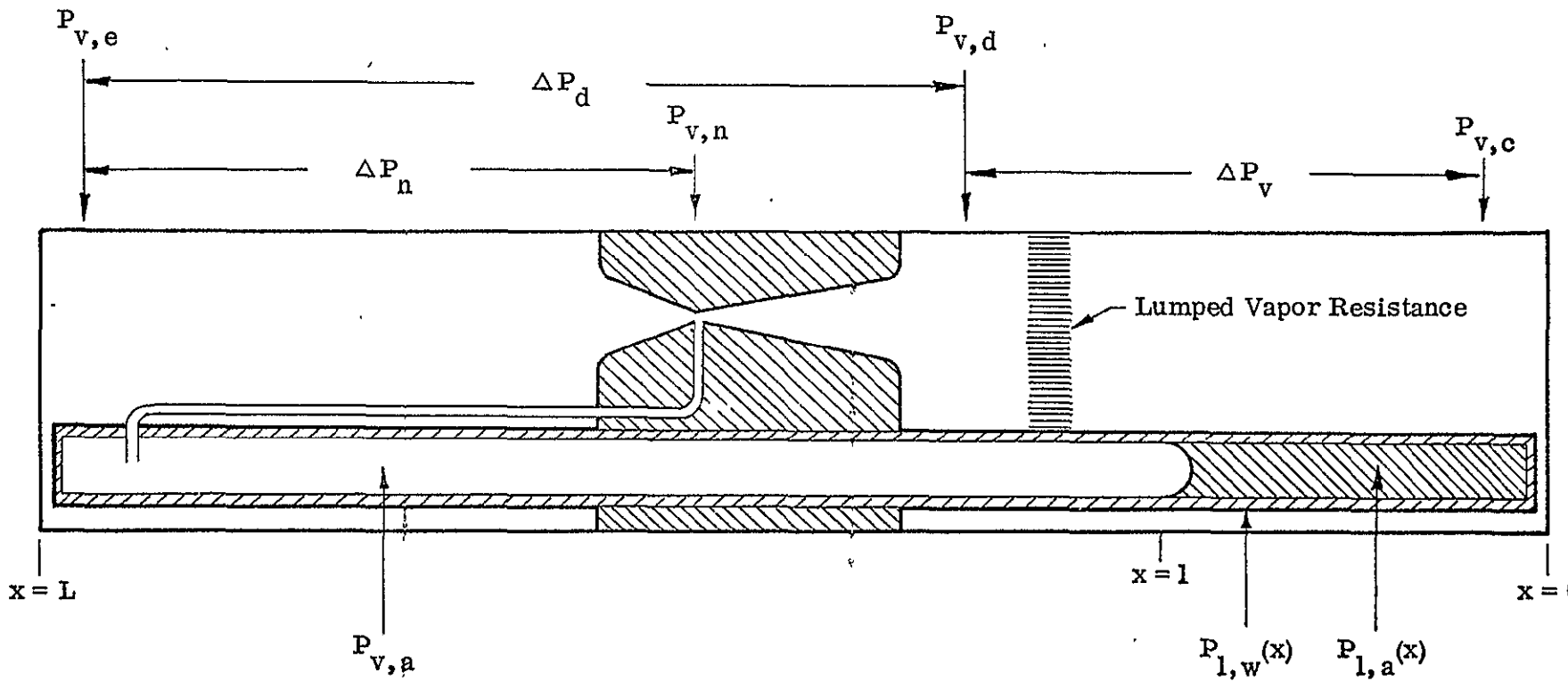


FIGURE 2.2
HEAT PIPE SCHEMATIC DEFINING TERMS USED IN THEORETICAL ANALYSIS

η is the product of nozzle and diffuser efficiencies and F is related to the throat area of the venturi:

$$F = \frac{1}{2 \rho_v \lambda^2 A_t^2 \eta_n} \quad (6)$$

where

ρ_v = vapor density

λ = latent heat of evaporation

A_t = area of the throat of the venturi (assumed to be small compared to the vapor area of the heat pipe)

η_n = nozzle efficiency

The viscous pressure drop of the vapor is given by:

$$\Delta P_v = \frac{F}{C_v} Q \quad (7)$$

where C_v is the inverse of the lumped vapor resistance.

Finally, the gravity term for a given elevation angle is:

$$\Delta P_{\text{grav}} = \rho_l g L \sin \alpha \quad (8)$$

Substitution of Equations 4, 5, 7, and 8 into 1 yields the complete pressure balance for this heat pipe. This pressure balance has not yet taken into account the suction provided by the jet pump. This will be done later in a separate "priming" equation. The venturi is included in the pressure balance only through its losses.

Before making the substitution, it is convenient to define some dimensionless parameters. Let $\Delta P_{\text{cap},o}$ be the maximum capillary pressure of the wick and let Q_o be the maximum heat transfer rate which can be achieved with a fully primed artery and in the absence of any other but viscous losses in the liquid. Then we get:

$$\Delta P_{\text{cap},o} = \frac{1}{C_a + C_w} L Q_o \quad (9)$$

We can also express the capillary pumping and the gravity term as dimensionless parameters:

$$f = \frac{\Delta P_{\text{cap}}}{\Delta P_{\text{cap},o}} \quad (\leq 1) \quad (10)$$

$$\delta = \frac{\rho_l g L \sin \alpha}{\Delta P_{\text{cap},o}} \quad (\leq 1) \quad (11)$$

Also

$$\gamma = \frac{C_a + C_w}{C_w} \quad (12)$$

Finally, a new nozzle parameter is defined as:

$$\Delta P_{\text{cap},o} = F_o Q_o^2 \quad (13)$$

F_o relates to a new throat area, A_o , in the same way as F , relates to the actual throat area A_t (Equation 6). Although A_o has been introduced only as a mathematical convenience, it does have a physical meaning. It is the throat area which would give a suction pressure equal to the capillary limit of the wick if the vapor flow corresponds to the previously defined Q_o . Because of Equation (6), the following relationship holds:

$$\frac{F}{F_o} = \left(\frac{A_o}{A_t} \right)^2 \quad (13a)$$

Making all these substitutions and neglecting the viscous losses in the vapor yields the following normalized pressure balance:

$$f = \delta + \left[\gamma \left(1 - \frac{1}{L} \right) + \frac{1}{L} \right] \frac{Q}{Q_o} + (1 - \eta) \left(\frac{A_o}{A_t} \right)^2 \left(\frac{Q}{Q_o} \right)^2 \quad (14)$$

In this equation, the terms δ , γ , η and A_o/A_t are design parameters of the heat pipe.

δ defines the orientation, γ the wick, η the venturi efficiency, and A_o/A_t the venturi geometry. The terms f , Q/Q_o , and l/L are operational parameters. f defines the actual capillary pumping, Q/Q_o the heat transfer rate, and l/L the percentage fill of the artery. The pressure balance Equation (14) states that for a given heat transfer rate Q/Q_o , the capillary pumping and the fill condition of the artery are not uniquely defined. A second equation is needed to define the system completely.

Since the interior of the artery and the throat of the venturi are connected, the following condition must also be satisfied:

$$P_{v,a} = P_{v,n} \quad (15)$$

The pressure of the vapor in the unfilled portion of the artery is constant along the length and related to the pressure of the liquid in the filled portion through:

$$P_{v,a} = P_{l,a} (l) + \Delta P_{cap,a} \quad (16)$$

Where $\Delta P_{cap,a}$ is the capillary pumping of the partially filled artery. (For a circular artery $\Delta P_{cap,a}$ is given by $4\sigma/D_a$). The liquid pressure is related to the condenser pressure through:

$$P_{l,a} (l) = P_{v,c} - \rho_l g l \sin \alpha - \frac{1}{C_a + C_w} l Q \quad (17)$$

The suction created at the throat of the venturi is the result of acceleration of the vapor in the converging nozzle. This pressure difference is proportional to the square of the velocity and can therefore be expressed as (Ref. 2):

$$P_{v,e} - P_{v,n} = F Q^2 \quad (18)$$

Where F is the proportionality constant defined in Equation (6). Equation (18) can be rearranged as follows:

$$P_{v,n} = P_{v,e} - F Q^2 = P_{v,c} + \Delta P_v + \Delta P_d - F Q^2 \quad (19)$$

Substituting the appropriate expressions for ΔP_v and ΔP_d in (19) and then entering (16), (17), and (19) into (15) gives the following "priming" equation:

$$\rho_l g L \sin \alpha + \left(\frac{1}{C_a + C_w} + C_v \right) Q - \Delta P_{cap, a} - \eta F Q^2 = 0 \quad (20)$$

This equation can be normalized in the same way as the pressure balance equation to yield:

$$\eta \left(\frac{A_o}{A_t} \right)^2 \left(\frac{Q}{Q} \right)^2 + \varepsilon - \frac{1}{L} \left(\delta + \frac{Q}{Q_o} \right) = 0 \quad (21)$$

Where ε is defined as:

$$\varepsilon = \frac{\Delta P_{cap, a}}{\Delta P_{cap, o}} \quad (22)$$

The pressure balance Equation (14) and the priming Equation (21) form the basis for determining the operation of the jet pump assisted artery.

2.3 Interpretation of Performance Equations

Typical solutions of the pressure balance and the priming equation are shown in Figures 2.3 and 2.4. In these figures notice the family of pressure balance curves for various values of f (the normalized capillary pumping). Values for f above 1 cannot be achieved, hence only the region to the left of the $f = 1$ curve represents possible states for the heat pipe to operate.

As the heat transport is increased, the artery begins to prime and the degree of priming is specified by the priming curve. Notice that, even at zero load, the artery is primed slightly. The amount of priming here is determined by capillary self-priming of the open artery against the gravity head.

For the example in Figure 2.3, the artery slowly primes as the relative heat transport increases from zero to .055. During this time, the capillary pumping requirement has been increasing up to 0.6 of its maximum value. As the heat transport is in-

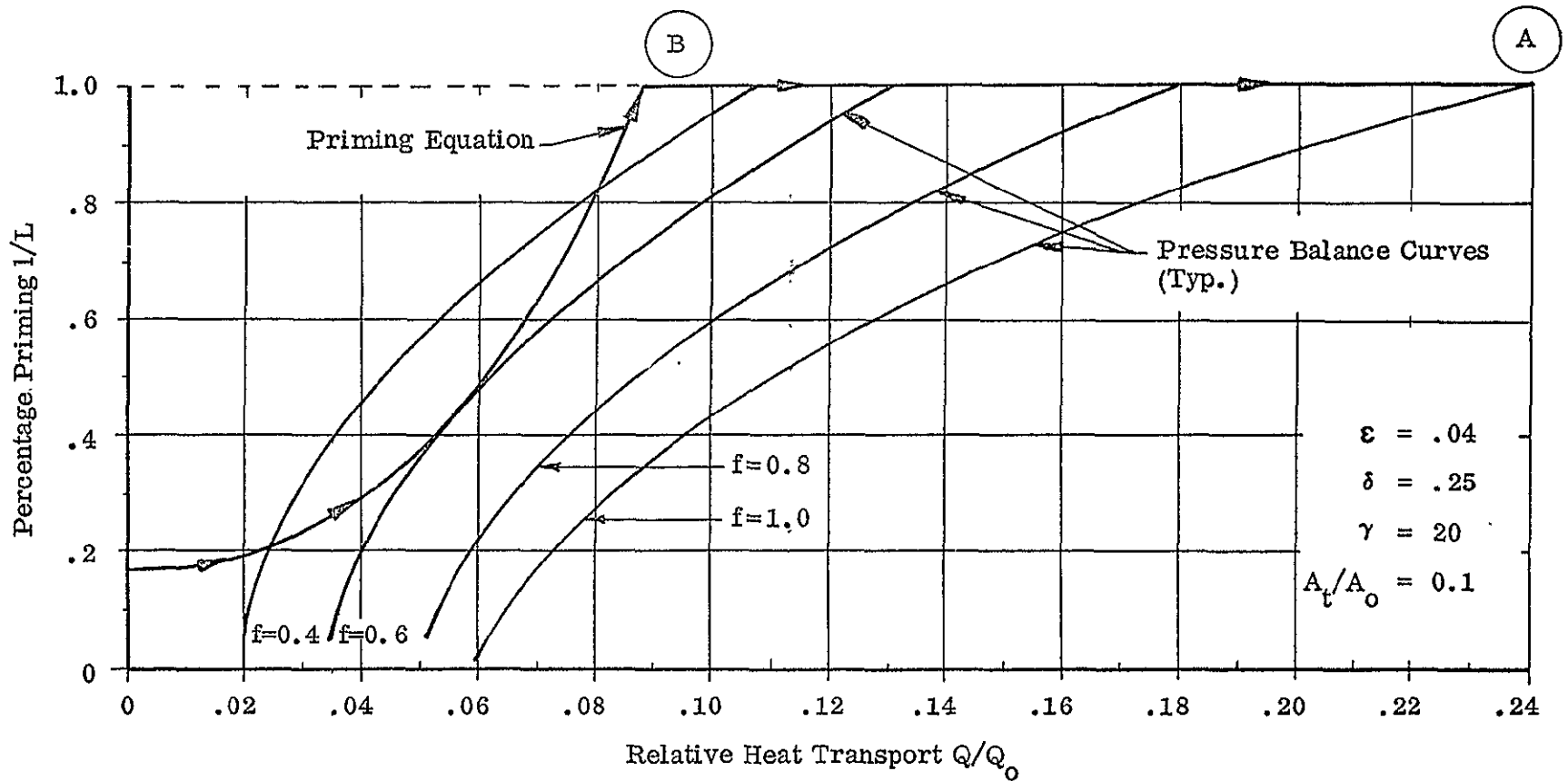


FIGURE 2.3
PLOTS OF PRIMING AND PRESSURE BALANCE EQUATIONS FOR A
DESIGN WHERE SELF PRIMING IS POSSIBLE

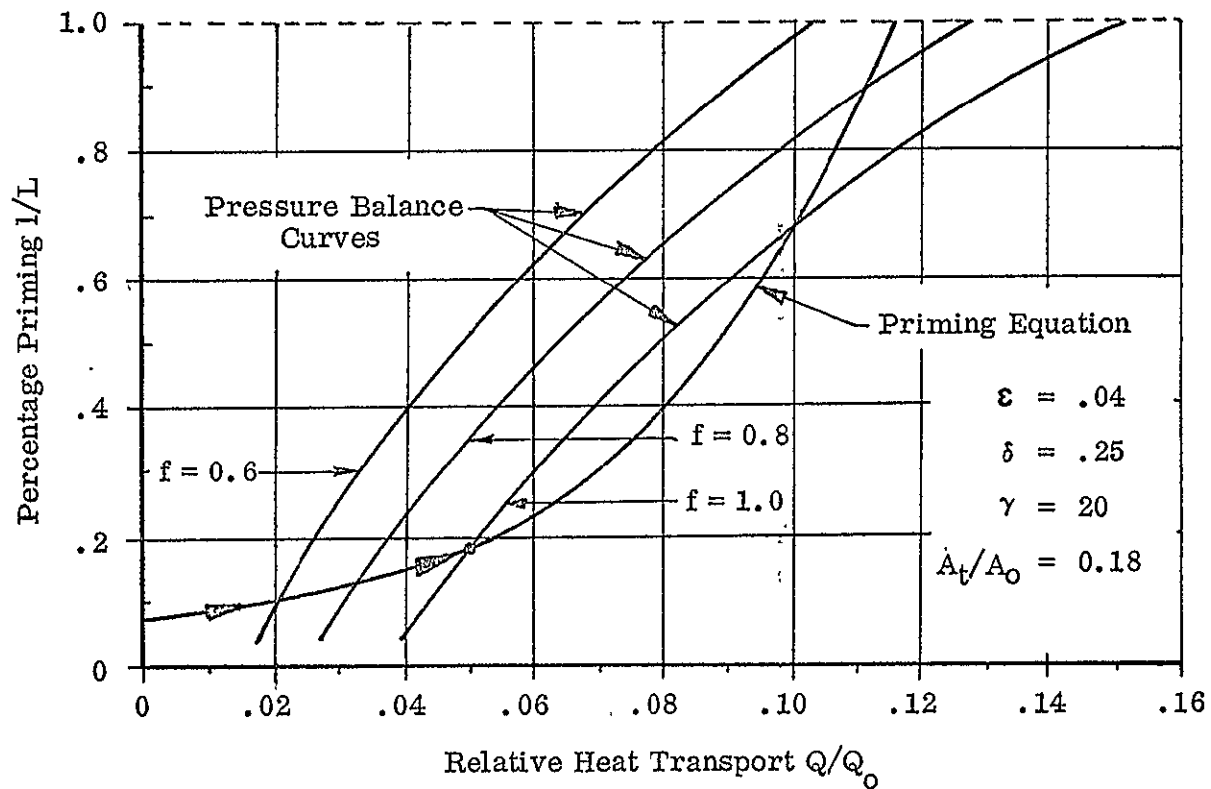


FIGURE 2.4
PLOTS OF PRIMING AND PRESSURE BALANCE EQUATIONS FOR A
DESIGN WHERE SELF PRIMING IS NOT POSSIBLE

creased further, the artery continues to prime until the artery is completely filled ($l/L = 1$). However, over this range of heat transport, the capillary pumping requirement is decreasing because, as the artery fills, the decreased liquid flow resistance more than compensates for increases in pressure drops in the jet pump, vapor, and elevation head. Hence, when the artery is filled, the capillary pumping requirement is less than 40% of capability. As the heat transport is increased further, the artery remains fully primed ($l/L = 1$) and the capillary pumping requirement increases until it reaches $f = 1$ at which point the maximum capillary pumping capability is reached. This point defines the maximum heat transport capability of the heat pipe for the specified conditions.

In Figure 2.4 the artery begins to prime as the heat transport is increased from zero. However, in this case, the capillary pumping requirement reaches a value of 1.0 before the artery is fully primed. For this heat pipe, the artery will never fully prime at the specified elevation and the relative heat transport capability is limited to .05. Notice that the pressure balance curve for $f = 1$ crosses the priming curve again so that, if this point could be reached, the artery could then be primed and the maximum heat transport would then be .15. This type of operation will be discussed in a later section of the report.

In order for the artery of a given heat pipe design to prime at a given orientation, the pressure balance curve for $f = 1$ and the priming curve must not intersect at all or, at most, at one point only. The optimized design occurs if the two curves are tangent to each other (just intersect at one point). The pressure balance equation for $f = 1$ and priming equation can be solved simultaneously to determine values for the design parameters when the two curves have one point of tangency. The results are shown in Figure 2.5 for a NH_3 heat pipe with 200 mesh pumping. The heat pipe is elevated 1.3 cm and the jet pump has an efficiency of 60%. The curves specify the minimum conductance of the priming wick (normalized with respect to the conductance of the artery) as a function of the dimensionless throat area ratio A_t/A_0 .

Figure 2.5 shows that the larger the throat area the larger the priming wick must be. Thus, in order to minimize the priming wick, a small throat should be used.

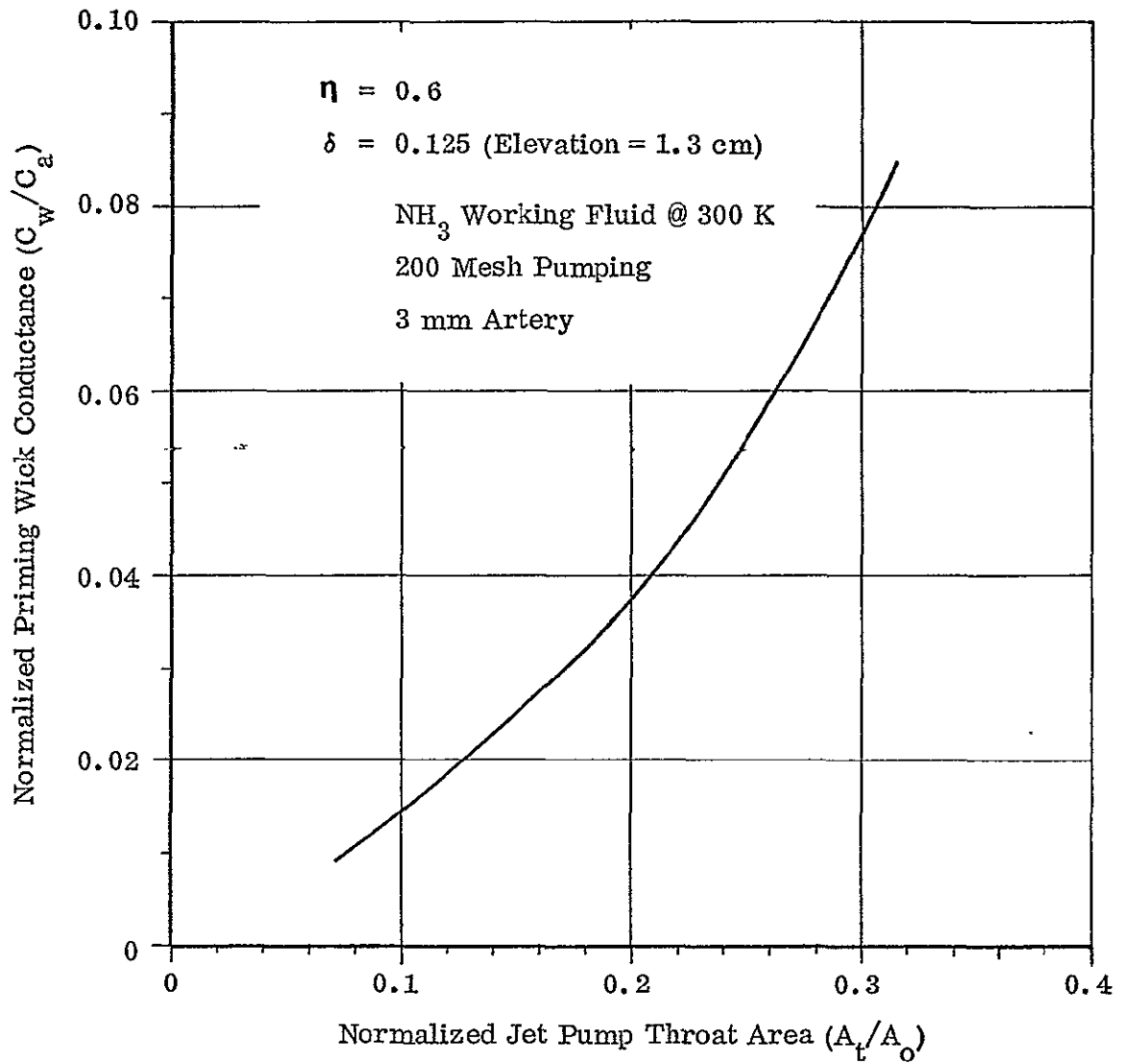


FIGURE 2.5
 MINIMUM PRIMING WICK REQUIREMENT AS A
 FUNCTION OF JET PUMP THROAT AREA

But if the throat area becomes too small, the vapor losses in the jet pump restrict the maximum heat transfer rate which the pipe can carry even with the artery fully primed.

When expressed in dimensionless form, the maximum heat transfer rate of the fully primed artery is independent of the conductance of the priming wick. This is seen by setting $f = 1$ and $l = L$ in the pressure balance Equation (14) which corresponds to point A in Figure 2.3. It can then be solved for Q/Q_0 as a function of A_t/A_0 . The results are given in Figure 2.6. It shows that Q/Q_0 decreases with smaller throat areas. The other curve in Figure 2.6 gives the dimensionless heat flow rate for which the artery is first primed (Point B in Figure 2.3). Either the set of Equations (14) and (21) or Figures 2.5 and 2.6 can be used to design a jet pump assisted arterial heat pipe. A sample design problem is given in the next section.

2.4 Application of Analytical Model to Design of Heat Pipe

Suppose a heat transport rate of 1,000 watts is required in a 1 m long heat pipe with an adverse elevation of 1.3 cm. The fluid shall be ammonia at 300 K and 200 mesh screen is to be used for artery and priming wick. The jet pump is assumed to have an efficiency of 60% and a nozzle efficiency of 90%.

Table 2.1 demonstrates how a design is arrived at. As a first try, an artery diameter of 3 mm is selected. Similarly, several values of A_t/A_0 are selected which hopefully span the required heat transport rate. For each value of A_t/A_0 , the required priming wick conductance ratio is found from Figure 2.5. The conductances C_a and C_w are the products of permeability and area for each wick. For the artery we have:

$$C_a = \frac{\pi}{128} D_a^4 \quad (23)$$

and for the priming wick:

$$C_w = A_w K_w \quad (24)$$

Where A_w is the wick area and K_w its permeability. Since the artery diameter is known,

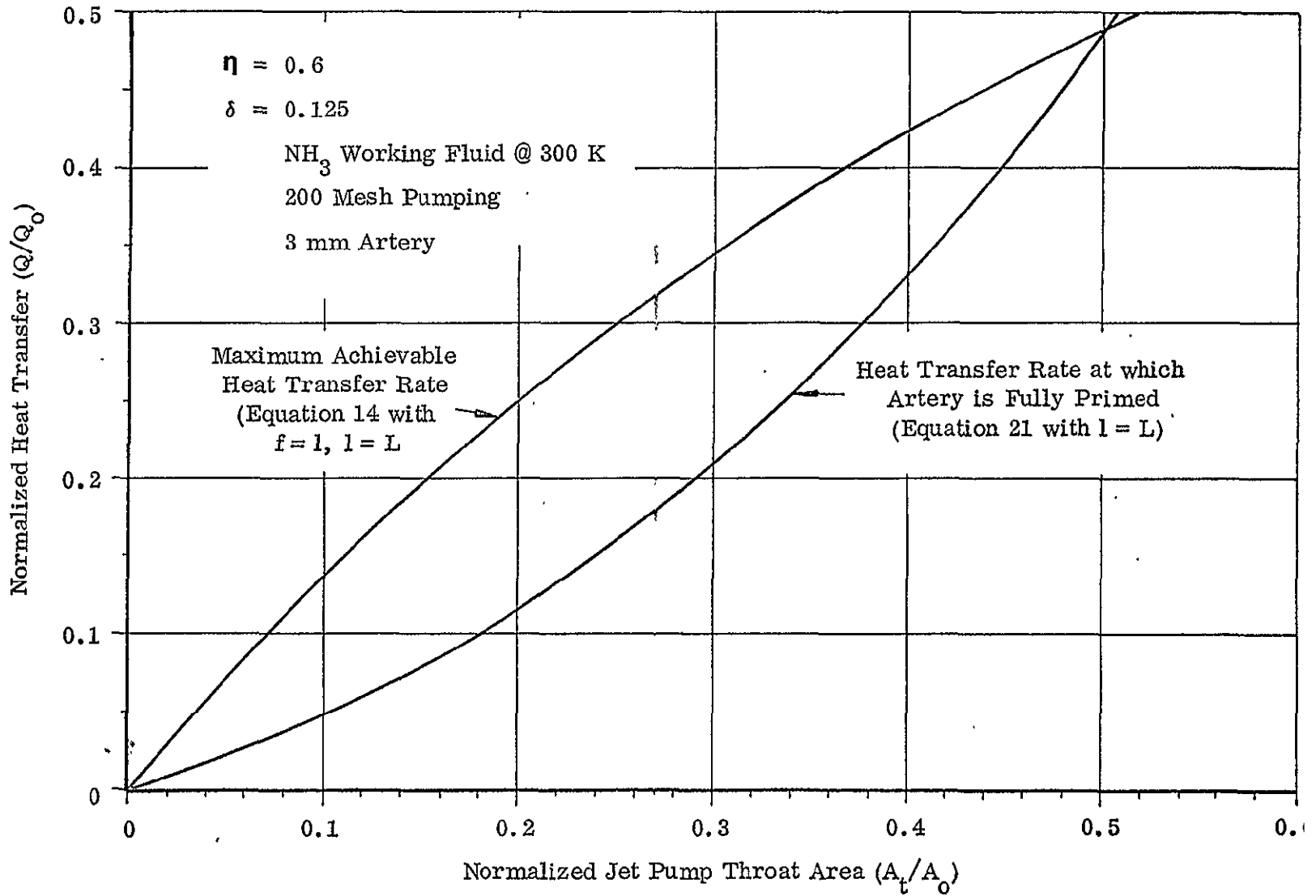


FIGURE 2.6
PERFORMANCE OF PRIMED ARTERY

A/A_o	C_w/C_a	$A_w K_w (m^4)$	$Q_o (KW)$	Q_{max}	Q_{prime}	$A_t (m^2)$	$D_t (mm)$
0.1	.0145	2.88×10^{-14}	4.13	0.56	0.19	3.56×10^{-6}	2.13
0.2	.375	7.46	4.22	1.06	0.49	7.26	3.04
0.25	.550	1.09×10^{-13}	4.29	1.29	0.68	9.25	3.43
0.30	.0765	1.52	4.38	1.52	0.92	1.13×10^{-5}	3.80

TABLE 2.1
ANALYTICAL DESIGN OF JET PUMP ASSISTED HEAT PIPE

$A_w K_w$ can be calculated for each case. It is listed in the third column of Table 2.1.

Q_o is determined from the expression:

$$Q_o = \frac{2 N_1}{r_p L} (C_a + C_w) \quad (25)$$

Where N_1 is the liquid transport factor of the working fluid and L is the effective length assumed to be 1.0 m for this case. The achievable Q_{max}/Q_o is determined from Figure 2.6 using the left of the two curves. The required Q_{max} of 1,000 watts occurs for a value of A_t/A_o of 0.2. The heat transfer rate at which the artery is fully primed is also obtained from Figure 2.6 (Right Curve). The throat area A_t is determined by combining Equations (6) and (13) along with values of A_t/A_o in Table 2.1. Finally, the nozzle diameter is determined from its area assuming a circular cross section. Examination of the $A_w K_w$ value for A_t/A_o equal to 0.2 leads to the conclusion that a simple, homogeneous wick is not practical for this case. For instance, if the homogeneous wick were to be made from the same mesh screen as is used for capillary pumping (200 mesh, $K = 5.5 \times 10^{-11} \text{ m}^2$), then the required area for the priming wick is 13.5 cm^2 . This area requirement is greatly reduced if a composite wick is employed. This approach was taken in the design of the actual prototype.

3. BENCH TESTS

During the previous program, a model of the jet pump was tested using air as the medium. The tests established the achievable suction pressures and the pressure losses in the nozzle and diffuser sections. During the current program, further tests were performed using the same jet pump model in order to:

- Investigate the effect of mass-injection on jet pump performance.
- Estimate the rate of mass-injection which is required to prime the artery.
- Determine the pressure losses between artery and injection port.

In addition, a bench test was conducted on the jet pump designed for the arterial heat pipe. Results of the above tests are presented in the following subsections.

3.1 Effects of Mass-Injection on Jet Pump Performance

The performance of the jet pump can be described by two parameters; i. e. , the attainable suction pressure difference at the throat and the overall pressure loss incurred by the driving (motive) fluid. It is convenient to define a jet pump efficiency which relates these two parameters:

$$\eta = 1 - \frac{\Delta P_d}{\Delta P_n} \quad (26)$$

Where ΔP_n is defined as $P_o - P_1$ (see Figure 3.1) which represents the useful suction pressure and ΔP_d is defined as $P_o - P_2$ which represents the overall pressure loss. It can be shown that η is related to the conventional nozzle and diffuser efficiencies by the simple relationship:

$$\eta = \eta_n \eta_d \quad (27)$$

The efficiency of a jet pump without mass-injection was measured in the previous program to be approximately 63%. This value is in good agreement with litera-

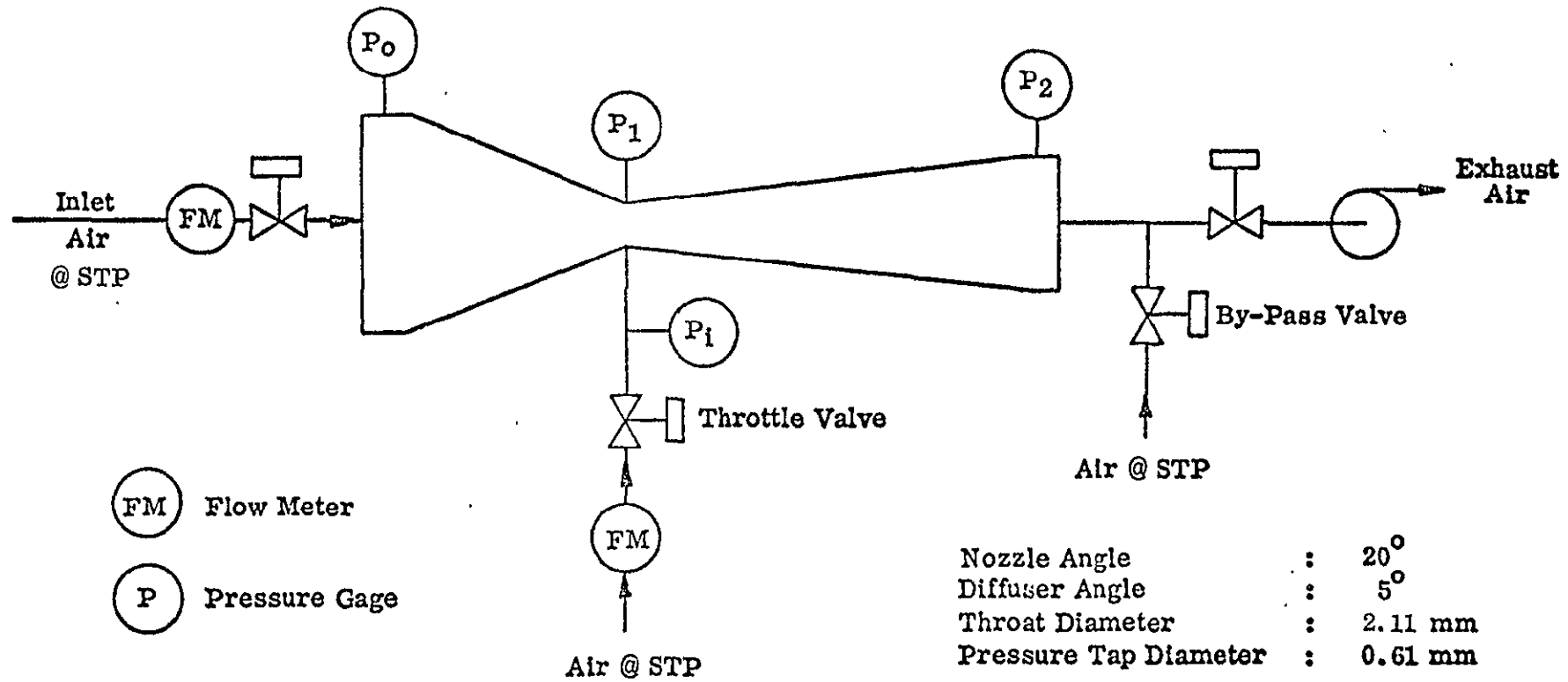


FIGURE 3.1 .

SCHEMATIC OF JET PUMP TEST SETUP WITH MASS INJECTION

ature data for the selected diffuser angle of 5 degrees (Ref. 3). The same basic test setup, which was used during the previous program, was now modified to measure the effects of mass-injection. This modified setup is shown schematically in Figure 3.1. The injected and the motive fluids were both air. The flow rate of the motive fluid was chosen to yield the same ΔP_n as ammonia vapor would give at a heat flow rate of 750 watts at 300 K. This value was used throughout this test program, and all injection flow rates are referenced to it. The results of the testing are given in Figure 3.2. It shows that, for relative injection rates of up to 5%, no degradation of efficiency is noticeable

3.2 Required Rate of Mass Injection for Artery Priming

After establishing the effects of mass-injection on performance, an estimate of the required rate had to be made. In order to prime the artery, the jet pump must be capable of ~~removing the vapor and/or noncondensable gas~~ from the artery within a reasonable time. This requires very little mass flow. For example, the total mass of NH_3 vapor contained in a typical artery of 3 mm diameter and 1 m length is about 0.1% of the mass of vapor flowing to the condenser in one minute at a heat flow rate of 750 watts. A second requirement for pumping is much more difficult to evaluate. During the priming process or when operating with a partially primed artery, the pressure inside the artery is slightly less than that of the surrounding vapor space. This condition necessitates a slightly lower temperature in the artery (because of saturation). Heat leaks will cause evaporation and will tend to restore equilibrium conditions within the artery. Thus, the jet pump must provide enough mass flow to offset this restoring mechanism. Rough estimates of the required vapor removal rate indicated very small mass flows. But since many assumptions went into these estimates, an experimental verification seemed desirable. Thus, the test setup shown in Figure 3.3 was devised. A mock-up of a typical artery was enclosed in a glass container which was partially filled with methanol. The artery was paralleled by a sight glass, and the necessary plumbing for evacuation of artery and container was provided. The pressure drop along a small capillary tube was used to measure the flow rate. After establishing equilibrium saturation conditions, the artery was

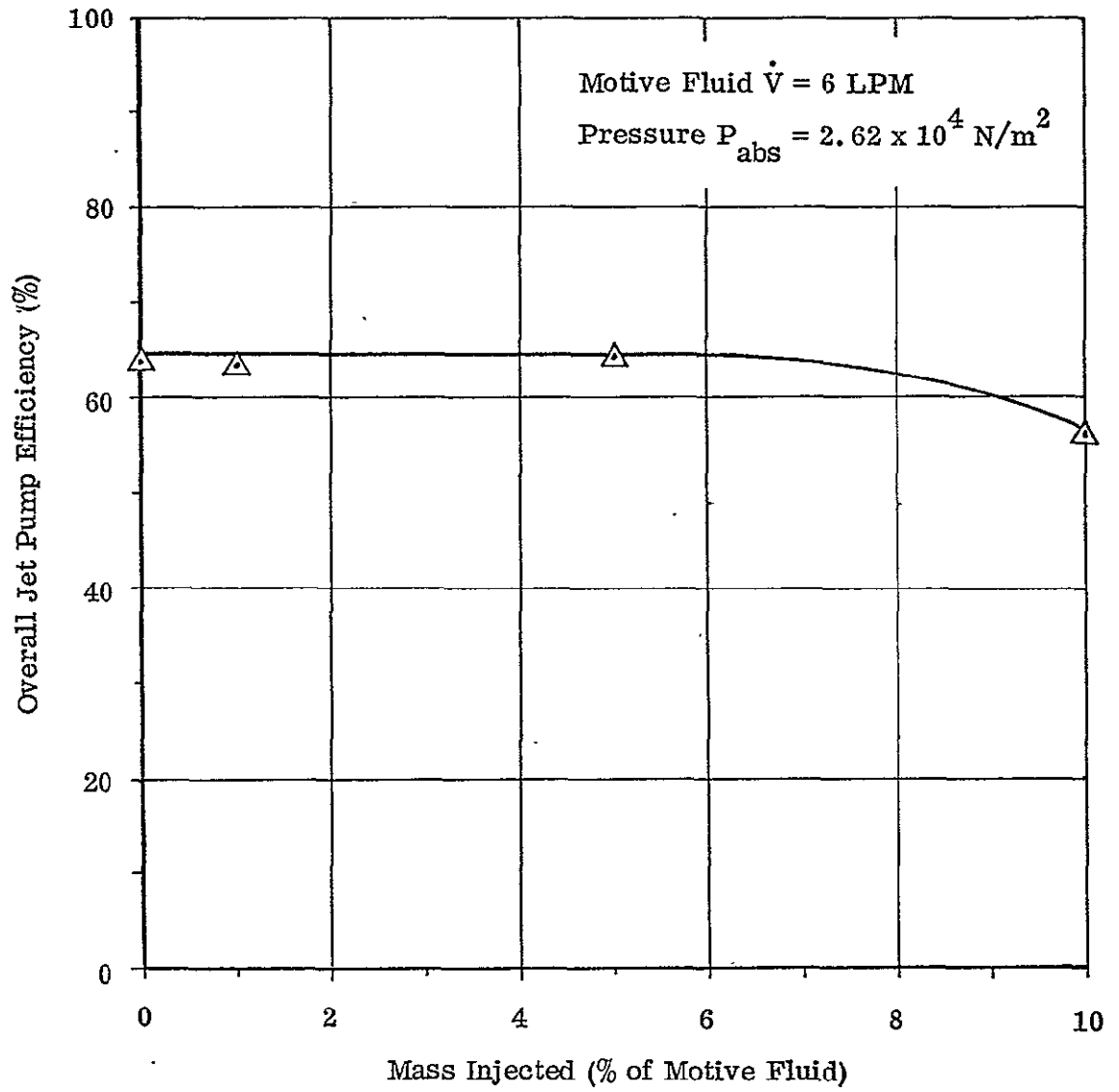


FIGURE 3.2
 EFFECT OF MASS INJECTION ON JET PUMP PERFORMANCE

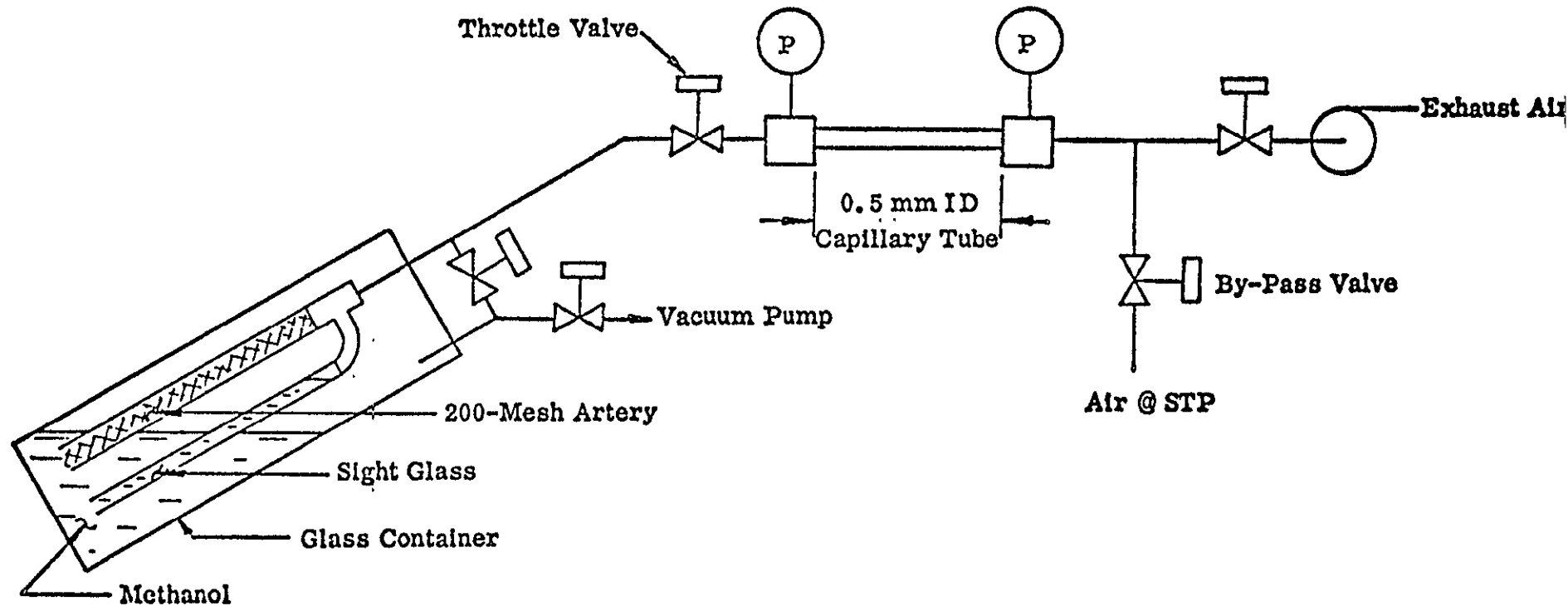


FIGURE 3.3
SCHEMATIC OF TEST SETUP FOR MEASURING
RATE OF VAPOR EVOLUTION FROM PARTIALLY PRIMED ARTERY

slowly primed by reducing the internal pressure. The intent was to maintain a partially primed state and to measure the rate at which vapor had to be pumped out. Actually, it proved difficult to hold the liquid level completely stable. Instead, data were taken while the artery was slowly priming. The required mass flow rate was below the limit of detection with the present instrumentation. This limit corresponds to about 0.1% of the NH_3 vapor flow rate with a heat input of 750 watts. Since the jet pump efficiency was found to be independent of injection up to mass flow ratios of 5%, the effects of mass-injection can be neglected in the design of the jet pump. It may be argued that the results obtained with methanol are not directly applicable to ammonia. But since the required mass flow rate is at least one order of magnitude below the threshold of affecting the jet pump's performance, the substitution of easy-to-handle methanol for the high pressure ammonia appears justified.

3.3 Pressure Losses Between Artery and Injection Port

Whenever there is mass flow between the artery and the jet pump, a pressure loss will occur in the connecting tube and in the injection port. Since this port has a very small diameter (~ 0.5 mm), the pressure drop could be substantial and would detract seriously from the useful suction pressure difference. Thus, a measurement of this pressure loss was performed on the bench model of the jet pump. The results are given in Figure 3.4. The pressure loss is expressed in percent of the useful suction pressure difference at the reference flow rate. Similarly, the injected flow rate is also normalized with respect to the reference flow rate. While the results are strictly applicable only to the bench model jet pump, a general conclusion can be drawn. The injected mass flow rate should be preferably less than 1% of the main vapor flow rate. Otherwise, substantial loss in useful suction could occur. It was this result which led to the experimental determination of the required injection flow rate which was described previously.

3.4 Bench Test of Prototype Jet Pump

After fabrication, the jet pump, which was to be used in the arterial heat pipe, was tested to measure its performance and to compare the results with the design analysis. A description of the design can be found in Section 4.

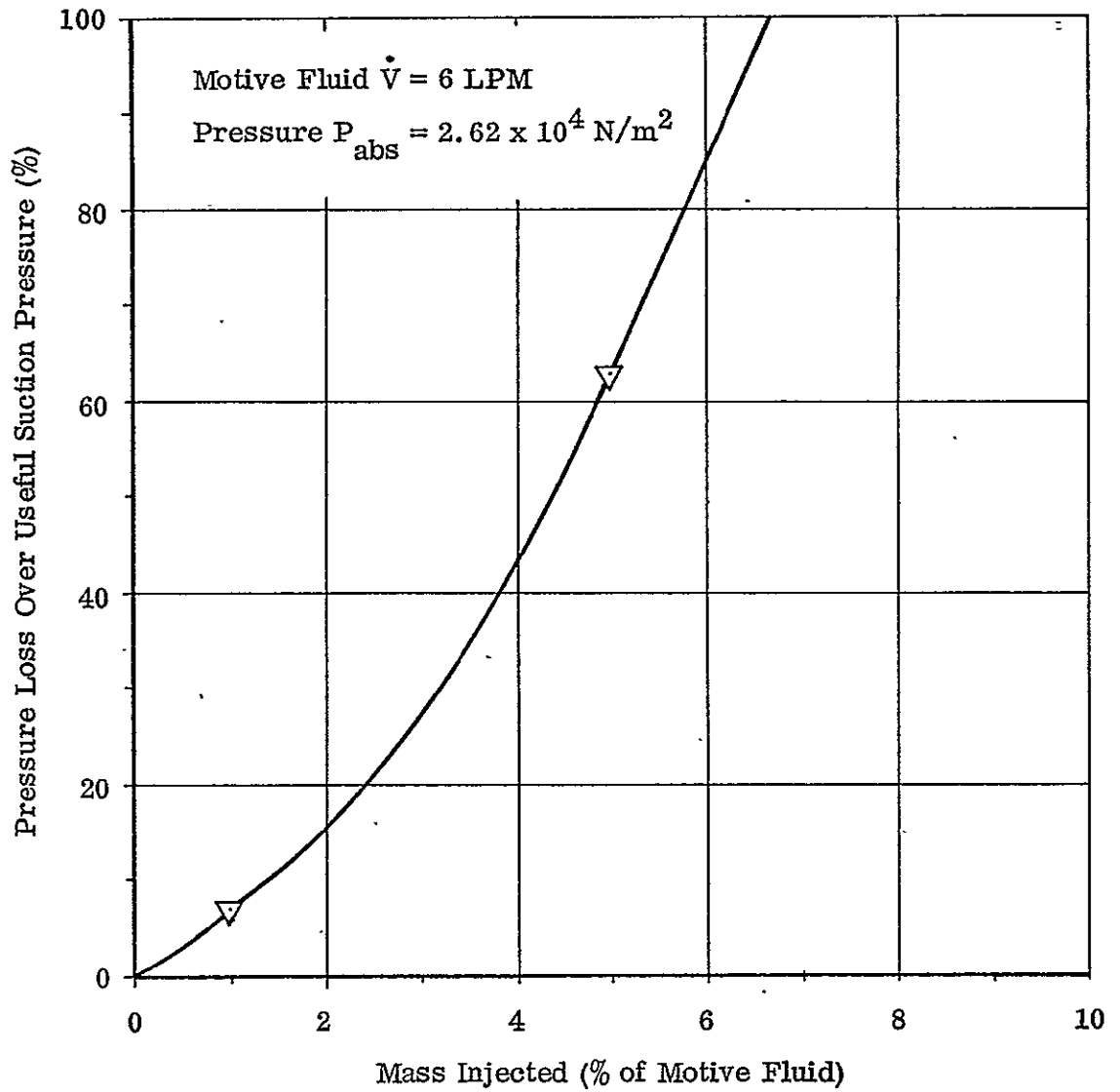


FIGURE 3.4
 PRESSURE LOSS OF THE INJECTION PORT

The jet pump was tested using air as the medium without mass-injection. The test setup was the same as shown in Figure 3.1 except that the injection line was not included in the present experiment. Results of the test are shown in Figure 3.5. The efficiency of the jet pump increases linearly up to a volume flow rate of 4 LPM and then the increase is much slower up to the maximum measured flow rate of 8 LPM. The jet pump was designed for a maximum heat transport of 500 watts in an ammonia heat pipe and to have an efficiency of at least 60%. The corresponding volume flow rate of air for the breadboard test, assuming the same nozzle pressure drop for both fluids, is 4.1 LPM at STP. At this flow rate, the measured nozzle pressure drop in Figure 3.5 is 1200 N/m^2 , the pressure loss across the jet pump is 550 N/m^2 , and the jet pump efficiency is 54%. Although it does not quite meet the design goal of 60%, the efficiency was judged acceptable. Actually, the measured suction pressure of the jet pump with air is about 30% higher than was predicted based on the geometrical throat area. This discrepancy has been seen before during tests with the previous jet pump and can be explained by the "vena contracta" effect within the throat.

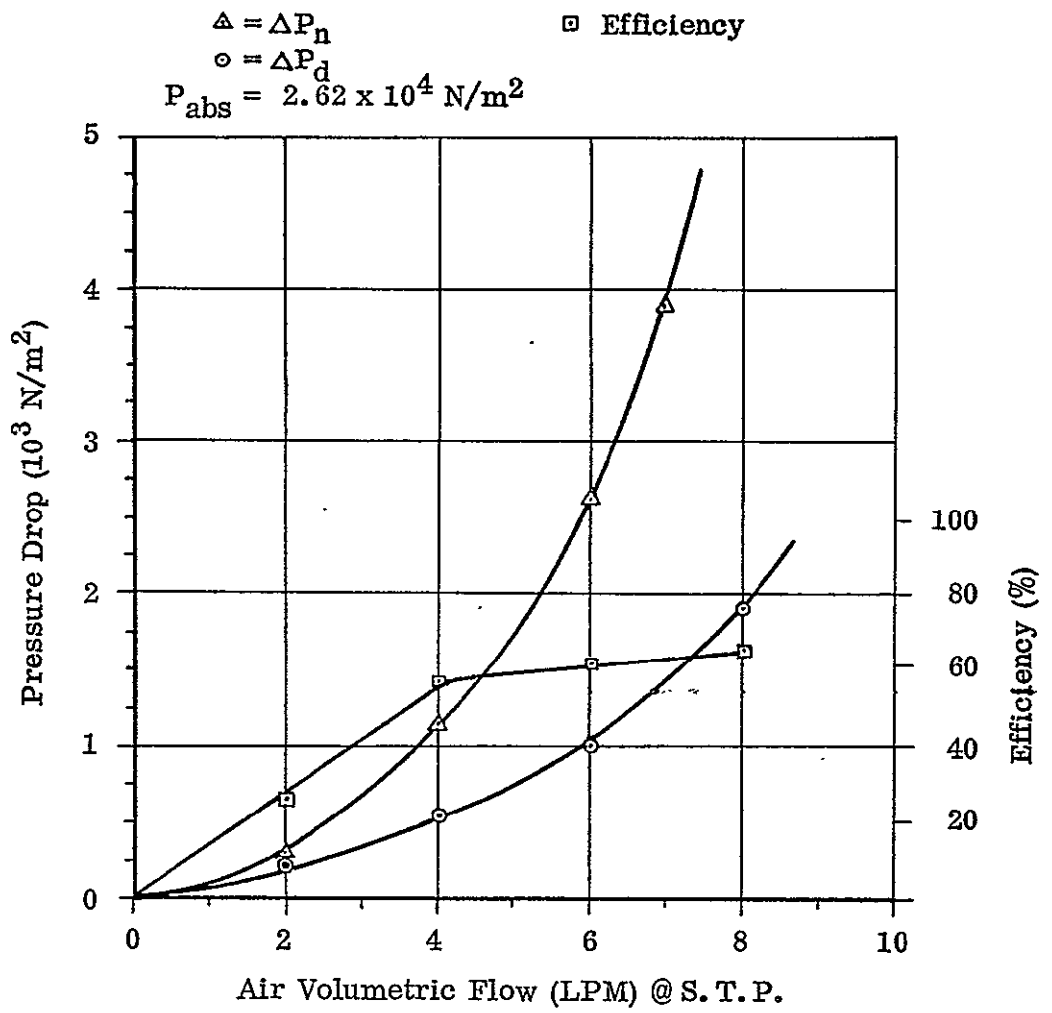


FIGURE 3.5
JET PUMP PERFORMANCE

4. DESIGN OF JET PUMP ASSISTED ARTERIAL HEAT PIPE

4.1 Thermal Design

A self-imposed performance goal for the prototype heat pipe was that it be able to prime at an elevation of 1.3 cm and transport 500 watts. The length was chosen to be 120 cm and the diameter 2.5 cm. Since conventional arterial heat pipes are most difficult to prime with ammonia as working fluid, ammonia was selected for the prototype.

The thermal design was based on the analytical model described in Section 2. An artery diameter of 3.0 mm was chosen and the capillary pumping was to be that of 200 mesh screen. The jet pump was assumed to have an overall efficiency of 60% and a nozzle efficiency of 90%. The analysis yielded the following optimum design parameters:

Maximum Heat Transport Capability at 1.3 cm Elevation	560 Watts
Power at Which Artery Will be Fully Primed	190 Watts
Throat Diameter of Nozzle	2.13 mm
KA Product of Priming Wick	$2.76 \times 10^{-14} \text{ m}^4$

This optimum design was defined as the one which requires the smallest KA product of the priming wick for the selected performance goals. However, even this optimum wick was relatively large. In fact, a homogeneous wick fabricated from 200 mesh screen would be impractical. Therefore, a composite wick was chosen. The wick was composed of 50 and 200 mesh screen with the 50 mesh screen having a cross-sectional area of 38.0 mm^2 .

The thermal design discussed thus far does not include any pressure drops associated with bridges or a secondary wick. Since the artery and priming wick had to be separated from the tube wall to eliminate possible boiling in those wicks, bridges and a secondary wick were required to supply fluid to the inside of the evaporator wall. To allow for the pressure drops in these distribution wicks, the maximum heat trans-

port had to be reduced slightly assuming these wicks also have a capillary pumping capability of 200 mesh screen. If the heat transport is reduced from 560 watts to 500 watts, the axial pressure drop decreases from 636 N/m^2 (pumping capability of 200 mesh screen) to 530 N/m^2 . Hence, a net pressure drop of 106 N/m^2 is now available for the distribution wicks. A design was chosen which consisted of two layers of 200 mesh against the evaporator wall and six bridges each composed of six layers of 200 mesh screen. At a heat transport of 500 watts, this wick design resulted in a liquid pressure drop of 68 N/m^2 which was less than the 106 N/m^2 available. Hence, the heat pipe was expected to transport slightly more than 500 watts when fully primed.

4.2 Mechanical Design

The heat pipe was constructed from stainless steel tubing having an O.D. of 2.54 cm and an I.D. of 2.35 cm. The evaporator and condenser lengths were each 20 cm with the overall length being 120 cm. The effective length for heat transport was therefore 100 cm. The jet pump housing was located in the adiabatic region 30 cm from the evaporator end. This housing was attached to the heat pipe tube using flanges and o-ring seals. Figure 4.1 shows the overall configuration of the jet pump assisted arterial heat pipe.

Details of the jet pump design are listed in Table 4.1. The jet pump housing was machined from aluminum. Figure 4.2 shows details of the housing. Beside the jet pump, a 9.3 cm diameter hole was placed in the housing to allow the artery and priming wick to pass through. A thin stainless steel sleeve was forced in one end of the hole so that the wick could be sealed at this point. The evaporator end of the artery was sealed to a 1.6 mm diameter stainless tube which was attached to the jet pump housing through a swagelok fitting. A small hole in the housing at this point connected the tube to the injection port. A valve mechanism was placed in this line so that the connection between artery and jet pump could be closed, if desired, for a specific test. In Figure 4.2 the valve is shown in the open position. To close the valve, the seal plug had to be removed to insert a second plug which closed off the injection port. Then the seal plug was reinstalled to prevent leakage of the working fluid.

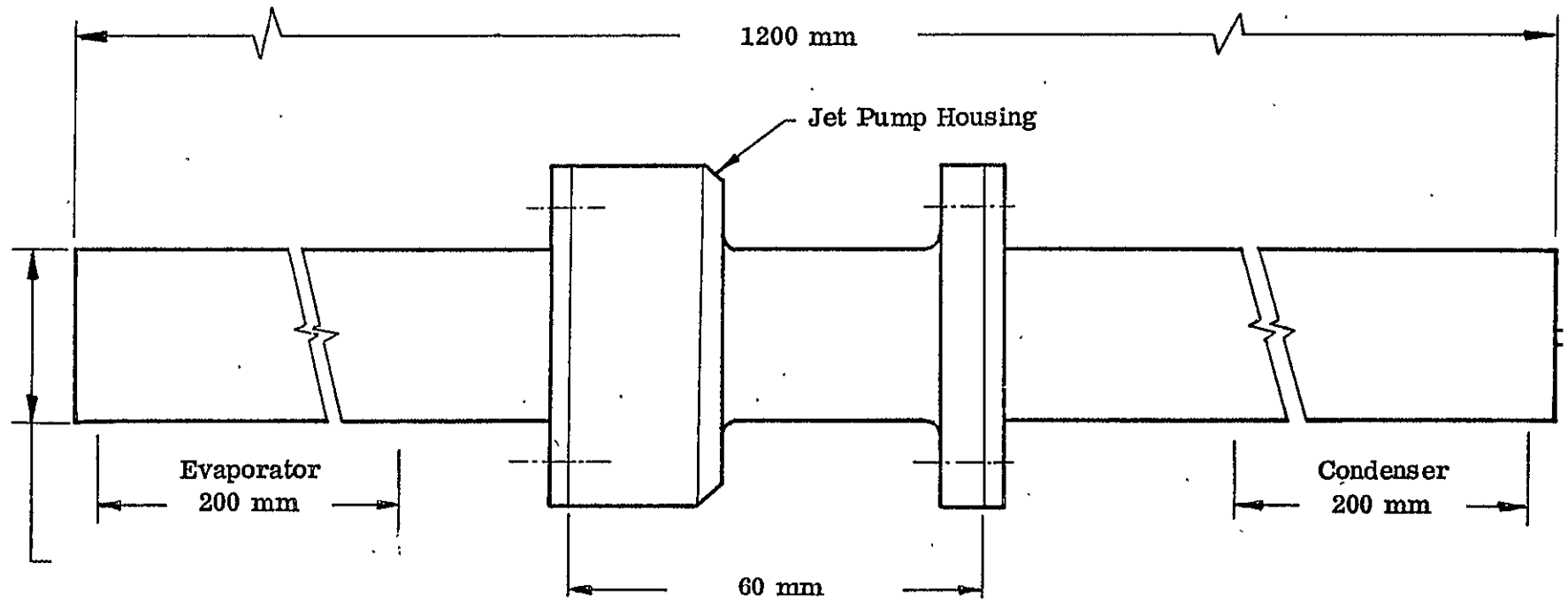


FIGURE 4.1
JET PUMP ASSISTED ARTERIAL HEAT PIPE DIMENSIONS

TABLE 4.1
JET PUMP DESIGN

Nozzle Inlet Diameter	:	6.35 mm
Nozzle Convergence Angle	:	20 ^o
Throat Diameter	:	2.13 mm
Diffuser Divergence Angle	:	5 ^o
Diffuser Exit Diameter	:	6.35 mm
Injection Port Diameter	:	0.61 mm

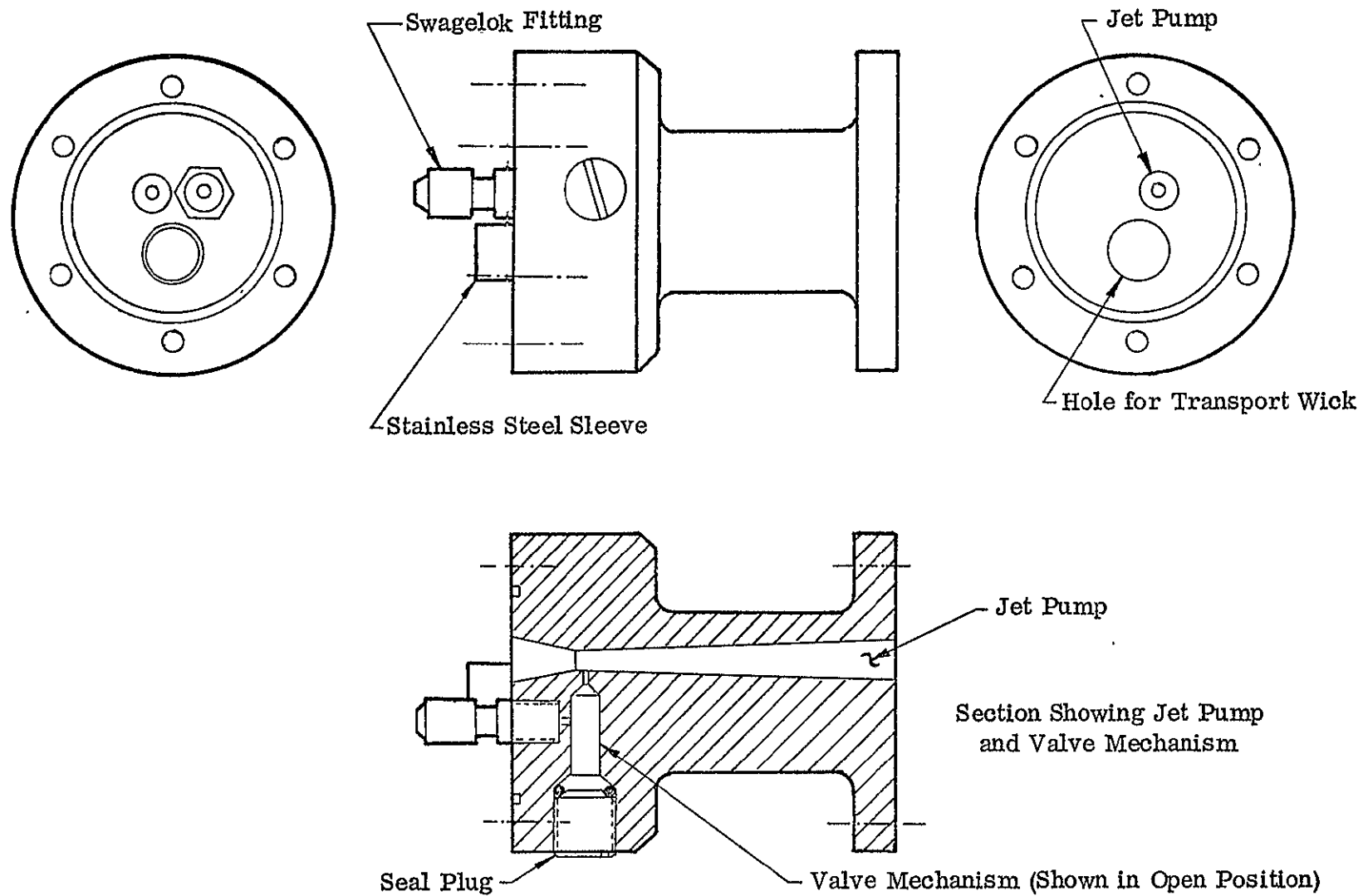


FIGURE 4.2
DETAIL OF JET PUMP HOUSING

The artery was formed from two wraps of 200 mesh screen having an inside diameter of 3 mm. Six layers of 50 mesh screen were then wrapped around the artery to form the priming wick. To provide the desired composite effect, two wraps of 200 mesh were placed over the 50 mesh and this screen was joined to the 200 mesh of the artery at the evaporator end. The artery was left open at the condenser end. At the point where the wick passes through the jet pump housing, the outer 200 mesh screen was sealed with more 200 mesh screen to the stainless steel sleeve. Figure 4.3 shows the wick configuration within the heat-pipe. In the condenser region, the priming wick was allowed to rest against the side wall of the tube which was first lined with one layer of 200 mesh screen. In the evaporator region, two layers of 200 mesh screen were placed on the inside wall of the tube. The bridge wicks in the evaporator, which were attached to the priming wick by spot welding, supported the priming wick away from the tube wall. These bridge wicks consisted of six wraps of 200 mesh screen shaped into a tube. Three tubes 20 cm long were attached to the priming wick at locations 120 degrees apart as shown in Figure 4.3. Contact between the tube bridges and the tube wall was provided by the spring force generated from forcing the wick inside the tube. The artery was thus elevated above the wall by 9.5 mm in the evaporator. This elevation correction was accounted for in all the test results discussed later.

4.3 Test Setup

After assembly, the heat pipe was charged with 38 grams of ammonia. Initial testing was performed with the jet pump disconnected from the artery so that the valve on the housing was closed before introducing the ammonia charge. Ten chromel-alumel thermocouples were attached to the heat pipe by spot welding. A heater wire was wrapped around the evaporator region. The evaporator and transport regions were insulated to minimize parasitic heat leaks. The condenser region was placed in a water bath so that the vapor during operation could be maintained at 300 K. Figure 4.4 is a schematic of the test setup. An adjustable support at the evaporator end was used to maintain the heat pipe orientation during a specific test. A valve was left on the fill tube so that the charge could be adjusted and helium introduced during later testing.

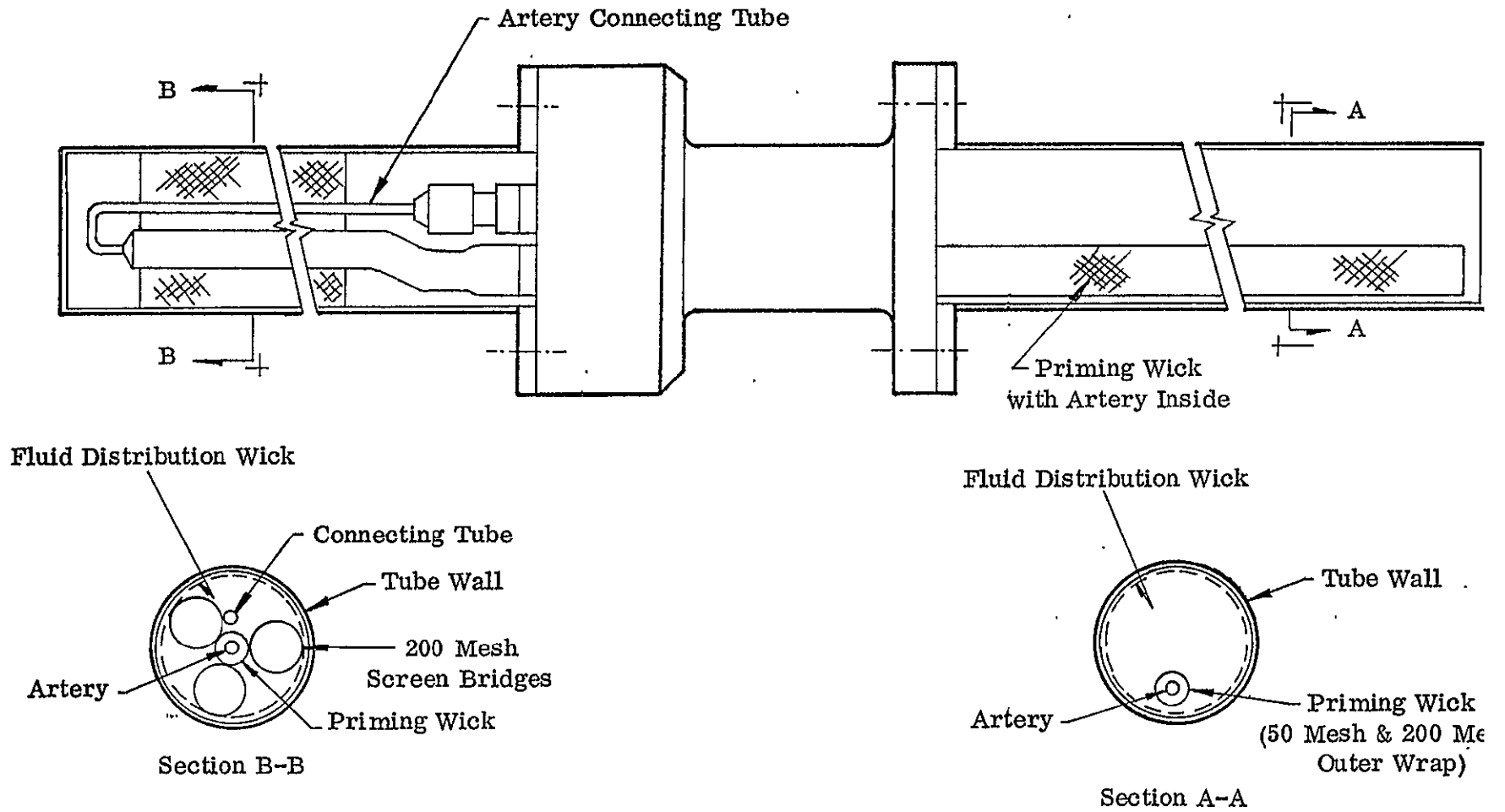


FIGURE 4.3
WICK CONFIGURATION

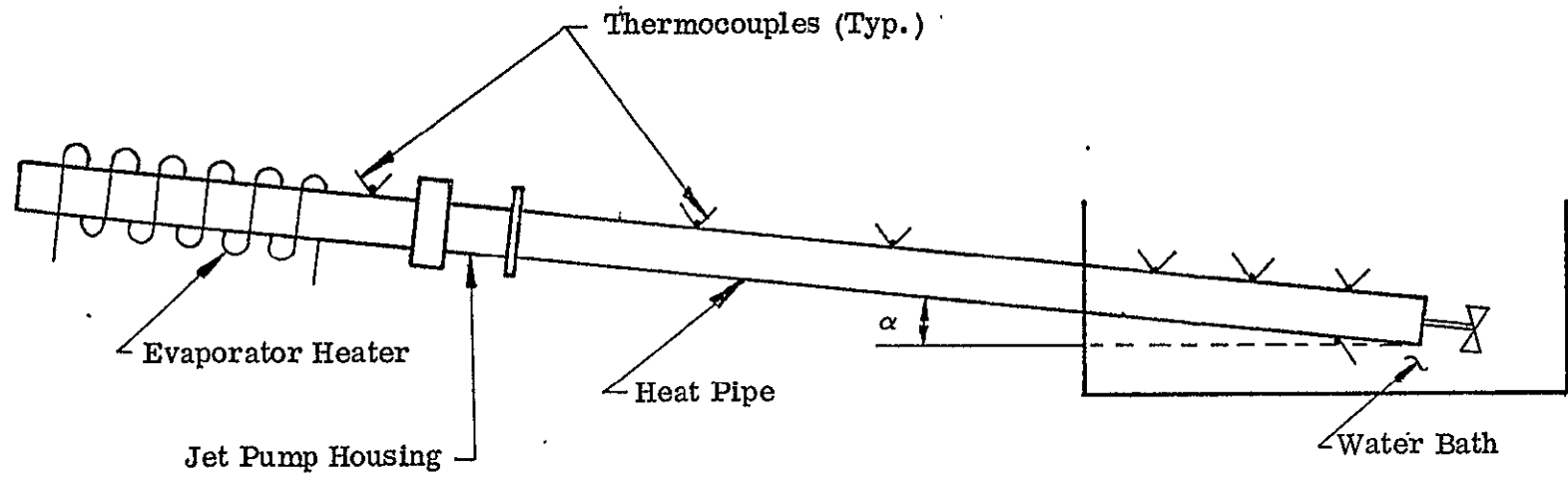


FIGURE 4.4
SCHEMATIC OF SETUP FOR TESTING
JET ASSISTED HEAT PIPE

5. TEST RESULTS WITH JET PUMP ASSISTED HEAT PIPE

The arterial heat pipe was tested in three different modes:

- (1) With the jet pump inactive
- (2) As a jet pump assisted arterial heat pipe with pure working fluid
- (3) As a jet pump assisted arterial heat pipe with noncondensable gas in the system

The results of the three tests are presented in detail in the following subsections.

5.1 Inactive Jet Pump

The first test mode was accomplished by closing the injection valve located at the injection port of the jet pump. Hence, the artery was completely denied of the benefit from the jet pump. For tests at each elevation, the artery was initially deprimed by raising the evaporator end more than 10 cm above the condenser, then bringing it back to 2.5 cm elevation to allow the coarse screen of the priming wick to fill before setting the heat pipe to the desired test elevation. This depriming procedure of the wick was adopted during all tests including those where the jet pump was activated. Likewise, during all tests the vapor temperature was maintained at 300 K. The results of the test with the closed injection port are shown in Figure 5.1 which shows a slightly better performance than predicted, at least at low elevations. This indicates that the artery was filling better than predicted, probably because the effective pumping radius was smaller than the design value. The predicted curve rises sharply at low elevations because of the contribution of the open artery.

5.2 Jet Pump Assisted Arterial Heat Pipe

The purpose of the second test was to demonstrate the transport capability of the jet pump assisted arterial heat pipe. The injection port was opened and the heat pipe was recharged with pure ammonia. Results were obtained for two different priming conditions:

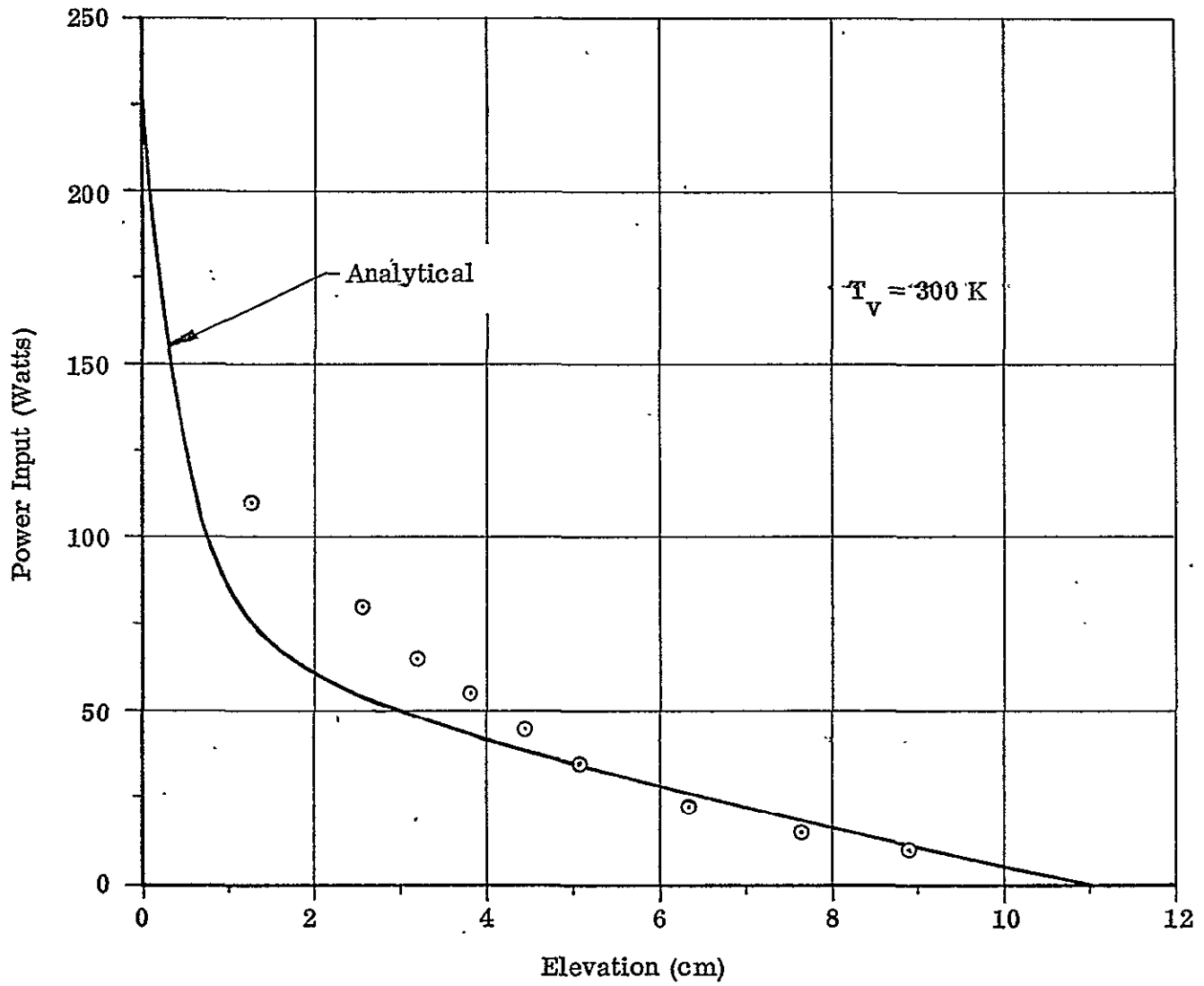


FIGURE 5.1
 PERFORMANCE OF JET PUMP HEAT PIPE
 WITH INACTIVE JET PUMP

- (1) Without pre-priming the artery
- (2) With pre-priming the artery

5.2.1 Without Pre-Priming the Artery

The heat pipe was set at a certain test elevation after going through the de-priming procedure discussed in Section 5.1. The heat input was gradually increased until a burnout was reached at each elevation. The test results are compared to predicted performance in Figure 5.2. Notice the very abrupt drop in heat transport capability at elevations above 2.0 cm. The heat pipe had been designed to provide priming of the artery at elevations of 1.3 cm and lower. From the data, it appears that the artery was actually capable of priming at elevations up to 2.0 cm. The portion of the analytical curve, which applies to tests without pre-priming the artery, follows the path ABCEF in Figure 5.2. The region below ABC is representative of the unprimed artery. Since the effect of the jet pump on priming the artery is negligible in this region, this curve corresponds very closely to the analytical curve for the case with the artery plugged (Figure 5.1). The curve is discontinuous from C to E along the dotted line. The region from E to F corresponds to the transport capability of the fully primed artery. An explanation for the remainder of the analytical curve shown in Figure 5.2 will be given later.

An interesting aspect of the results at elevations of 1.9 cm and lower was the recovery of the heat pipe after reaching burnout. The pipe could be recovered by lowering the power input by about 50%. This was unexpected since the jet pump should become ineffective once the artery dries out. In order to investigate the type of failure during burnout, a separate test was conducted. The heat pipe was operated at a constant heat input of 320 watts and 1.3 cm elevation (at this condition the artery is fully primed). Once the heat pipe reached a stable condition, burnout was induced by raising the evaporator 15 cm and then quickly lowering the heat pipe back to 1.3 cm elevation as soon as burnout occurred. This procedure forced the artery to deprime. After lowering the pipe to 1.3 cm elevation, the heat pipe did not recover. From this test result, it was concluded that the burnouts observed at elevations below 2.0 cm did not result in depriming of the artery. Instead, the burnout (condition where maximum

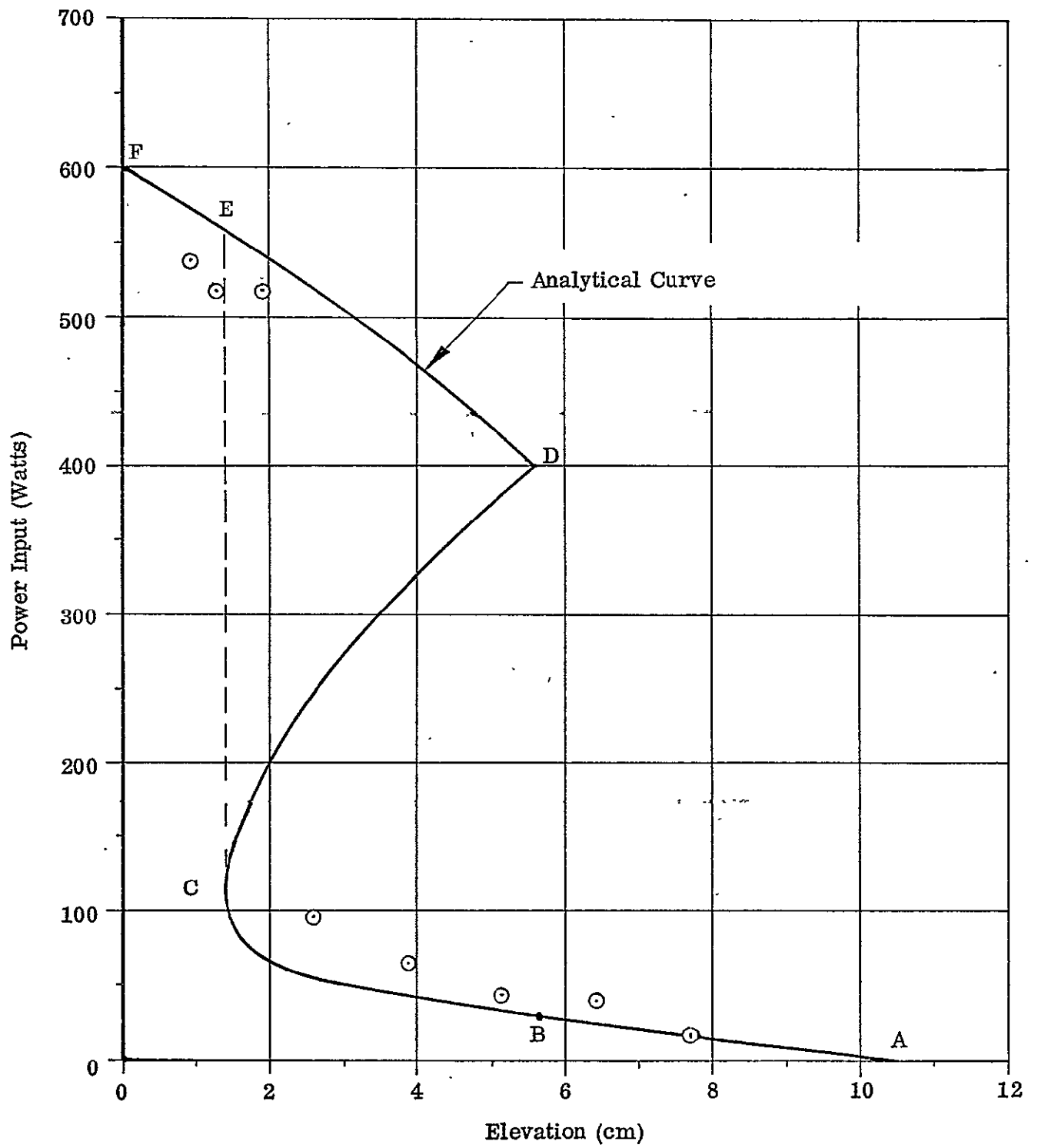


FIGURE 5.2
 PERFORMANCE OF JET PUMP ASSISTED HEAT PIPE
 WITHOUT PREPRIMING THE ARTERY

capillary pumping capability is exceeded) probably occurred in the secondary wick at the evaporator wall or in the bridge wicks connecting the axial wick with the secondary wick.

5.2.2 With Pre-Primed Artery

The range of heat transports and elevations, which is bounded in Figures 5.2 by sections CD, DE, and EC of the theoretical performance curve, cannot be reached without pre-priming the artery. Pre-priming can be achieved, for instance, in the following manner: The heat pipe is at first operated at an elevation of less than 2.0 cm and then the heat input is increased to, for example, 400 watts (at which point the artery is fully primed but not at its limit). The elevation can then be increased while holding the heat input constant. This corresponds to moving horizontally to the right in Figure 5.2. The elevation can be increased until reaching the limit corresponding to the analytical curve. This procedure was followed and the results are shown in Figure 5.3. The results definitely demonstrate that stable operation exists for conditions which cannot be reached except by pre-priming the artery. However, the maximum heat transport capability does not agree well with the analytical curves. More experimental results are needed to better understand this mode of operation.

The explanation for the shape of the analytical curve can best be understood using the diagrams of Figure 5.4. The five diagrams shown in the figure present the pressure balance and priming curves for various elevations (see Section 2). Only the pressure curve for $f = 1$ (maximum capillary pumping) is shown. However, it should be remembered that similar pressure balance curves exist for values of $f < 1$ and they all lie to the left of the curve $f = 1$.

Looking at the first diagram for an elevation of 0.5 cm, it is seen that the artery can prime by following the priming curve to $l = L$. But the heat pipe can transport more power by then moving horizontally to the point where the pressure balance curve crosses $l = L$. This maximum heat transport, Q_m , corresponds to a point on the analytical curve of Figure 5.2 between E and F. It can be reached by simply increasing the power from zero to Q_m .

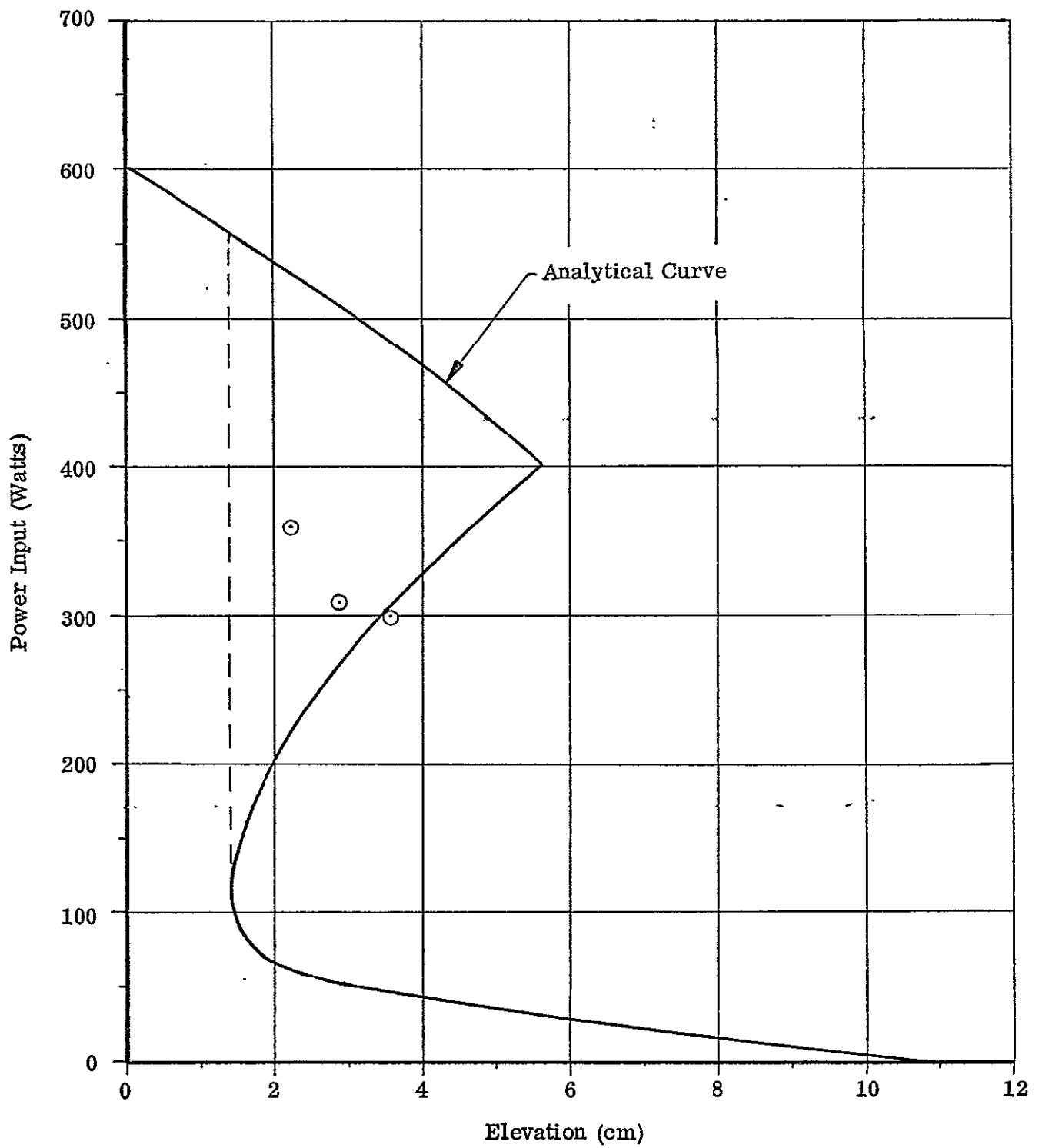


FIGURE 5.3
 PERFORMANCE OF JET PUMP ASSISTED HEAT PIPE
 WITH PREPRIMED ARTERY

In the second diagram of Figure 5.4, at an elevation of 1.4 cm, the heat pipe again can prime by following the priming curve to $l = L$. At the point where the two curves just touch, the heat transport, Q_u , corresponds to point C in Figure 5.2. Again after priming, the heat transport can be further increased to Q_m which corresponds to position E in Figure 5.2.

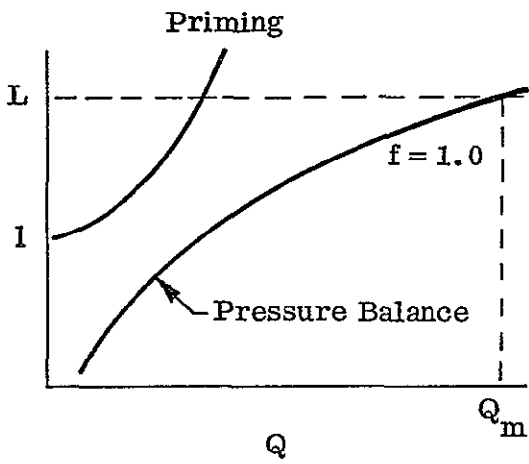
In the third diagram of Figure 5.4, the heat pipe cannot prime by simply increasing the power. The heat transport can only be increased to Q_u (corresponding to a point on the curve BC in Figure 5.2) at which point the maximum pressure balance is achieved. However, other conditions are valid if they can be reached. Heat transport from Q_p to Q_m does not violate the priming or pressure balance relationships. Point Q_p corresponds to a point between C and D in Figure 5.2, and Q_m corresponds to a point between D and E of the same figure. These test conditions are those described in this section where the artery must be first pre-primed at a low elevation before moving into conditions of higher elevation.

The fourth diagram in Figure 5.4 is similar to the third one. The heat transport, Q_u , corresponds to the point B in Figure 5.2. The heat transport, Q_m , must be reached by pre-priming the artery at lower elevation; and, since both the priming and pressure balance curves intersect at $l = L$, this point, Q_m , corresponds to D in Figure 5.2.

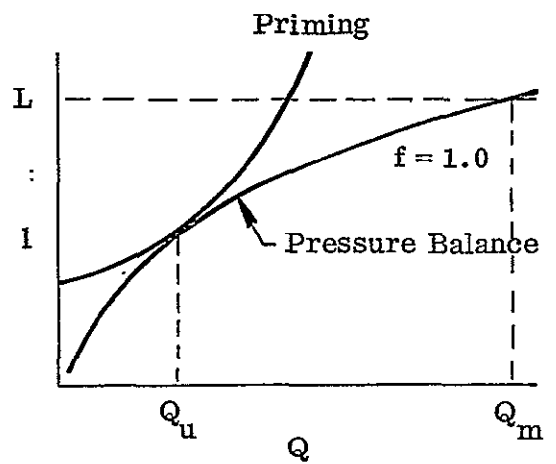
The last diagram in Figure 5.4 corresponds to elevations which are so high that only heat transports less than Q_u (corresponding to points on curve AB of Figure 5.2) can exist. Above Q_u the priming curve always represents a larger heat transport than the pressure balance curve including values for $l = L$, thus they cannot exist.

5.3 Jet Pump Assisted Arterial Heat Pipe with Noncondensable Gas

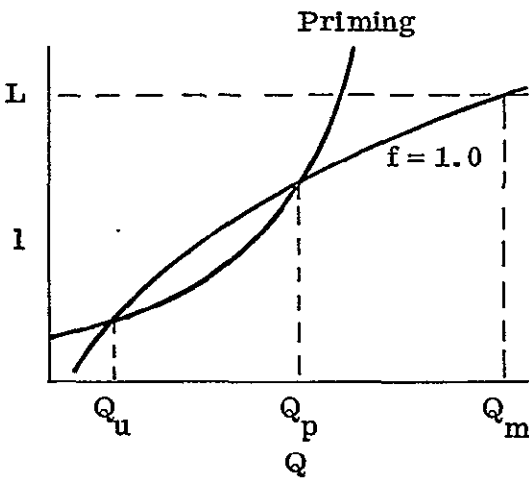
To demonstrate the feasibility of operating the jet pump assisted arterial heat pipe in the presence of noncondensable gas, 4.63×10^{-3} moles of helium were introduced into the heat pipe. This gas charge was sufficient to block about 25% of the condenser at 300 K. The heat pipe was tested in the manner described in Section 5.2.1, i. e., without pre-priming. The results are shown in Figure 5.5. The same



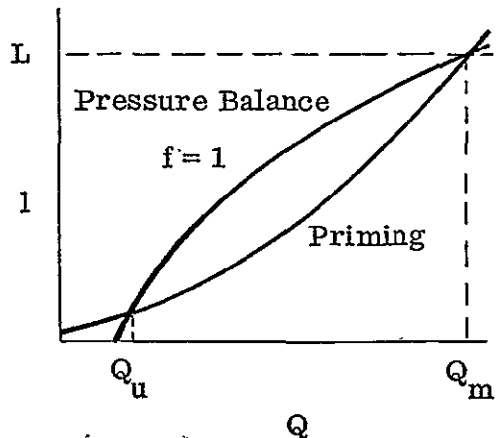
a. Elevation - 0.5 m



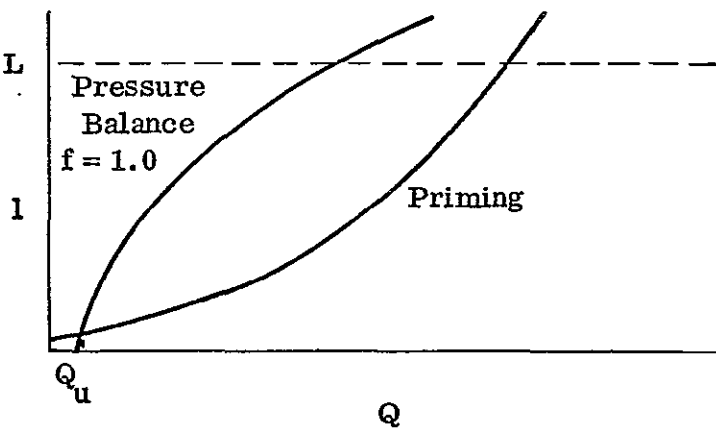
b. Elevation - 1.4 cm



c. Elevation - 3 cm



d. Elevation - 5.6 cm



e. Elevation - 7 cm

FIGURE 5.4

PRESSURE BALANCE AND PRIMING CONDITIONS FOR A JET PUMP ASSISTED ARTERIAL HEAT PIPE AT SEVERAL ELEVATIONS

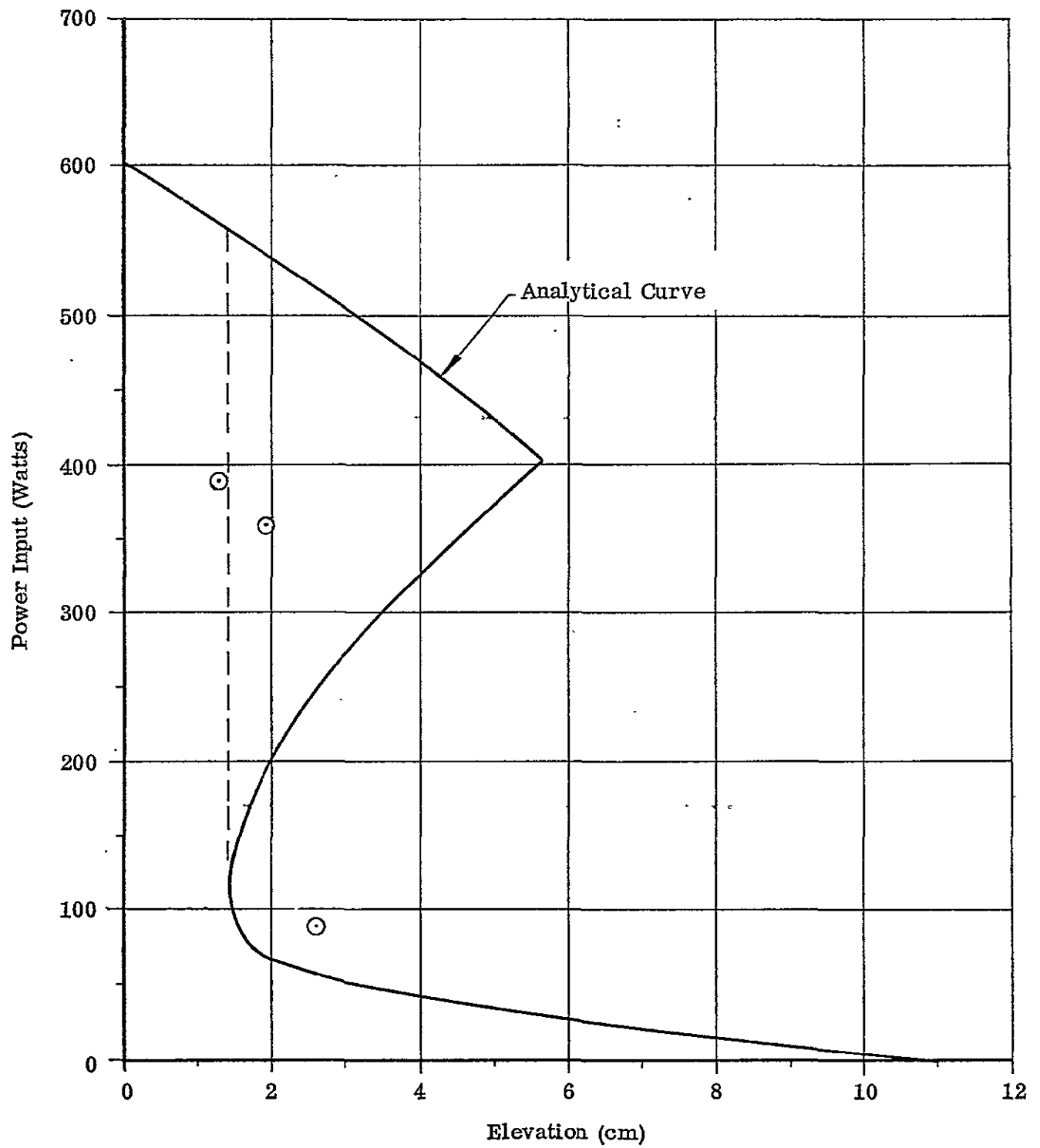


FIGURE 5.5
 PERFORMANCE OF JET PUMP ASSISTED HEAT PIPE
 WITHOUT PREPRIMING ARTERY AND WITH HELIUM IN HEAT PIPE

abrupt drop in heat transport capability occurs at elevations above 2 cm. But the heat transport capability at elevations below 2 cm is not as high as was measured without the noncondensable gas. Similar observations have been made in the past with tests of variable conductance heat pipes (Ref. 4). Tests before introducing the noncondensable gas show greater heat transport capability than with the gas present. The onset of boiling is well known to be affected by the presence of gas (Ref. 5) which may be the reason for the lower transport in the presence of gas observed in this heat pipe. Unfortunately, very little effort could be spent on measuring the performance with noncondensable gas present. This is one of the areas where additional work is needed.

6. CONCLUSIONS AND RECOMMENDATIONS

An analytical model of a jet pump assisted arterial heat pipe has been presented. Based on this model, a heat pipe incorporating a jet pump was designed which would prime at an adverse elevation of 1.3 cm and, when primed, would transport 500 watts. This heat pipe was manufactured and tested to meet these requirements. In fact, the heat pipe was capable of priming at elevations up to 1.9 cm and transported slightly over 500 watts. To verify that this capability was due to the jet pump, tests were conducted with the jet pump disconnected from the artery. In this case, the heat pipe was capable of transporting only about 100 watts which agrees well with predictions. Tests were also conducted to demonstrate the reliability for priming the artery in the presence of large quantities of noncondensable gas. Again the artery primed reliably.

The goals of this development have been conclusively demonstrated. When operated at elevations less than 1.9 cm, the heat pipe functioned as though it contained a homogeneous wick but with the transport capability of an arterial wick. This indicates that no special priming procedure is required for start-up or for recovery from a burnout. It is recommended that further testing be done with the heat pipe to better understand the operating modes of the system both with and without the presence of noncondensable gas. Then an experiment incorporating the jet pump in an NH_3 arterial VCHP is a logical next step toward the development of the system for flight applications.

It has been proposed that the artery can also be primed "inertially"; i. e., by providing sufficient fluid inventory in the evaporator to achieve priming quickly and without having to rely on liquid flow through the priming wick. The advantage of this technique is that the conductance of the priming wick can be reduced significantly so that a homogeneous wick can be used. However, this design will result in new operating characteristics which will probably be more restrictive than those found for the present design. The fabrication and testing of a heat pipe using this priming concept is also a desirable task for further development.

REFERENCES

1. Anderson, W. T., Edwards D. K., Eninger, J. E., Marcus, B. D., "Variable-Conductance Heat Pipe Technology - Final Research Report," NASA CR-114750, March 1974.
2. "Final Report for Jet Pump Assisted Artery," Dynatherm Corporation Report No. DTM-75-6, October 31, 1975.
3. Dudzinski, T. J., Johnson, R. C., Krause, L. N., "Venturi Meter With Separable Diffuser," Transactions of the ASME, Journal of Basic Engineering, March 1969.
4. "Technical Summary Report for Fabrication and Testing of Electrical Feedback Controlled Heat Pipes," Dynatherm Corporation Report No. DTM-76-4, June 22, 1976.
5. S. W. Chi, "Heat Pipe Theory and Practice," by Hemisphere Publishing Corporation, 1976.

dynatherm
CORPORATION



Marble Court and Industry Lane
Cockeysville, Maryland 21030
Phone (301) 666-9151